associated carcinogenesis, especially in the early stages of chronic hepatitis.

pSmad3L Prominence in Hepatocytic Nuclei in Proportion to Plasma HBV DNA Levels. Because HCC risk is related to plasma HBV DNA levels and chronic inflammation,[24] we next investigated the correlation of hepatocytic pSmad3L positivity with plasma HBV DNA levels and necroinflammatory activity in chronic hepatitis B patients (Fig. 2). Positivity of hepatocytic nuclei for pSmad3L in chronic hepatitis B specimens gradually increased in proportion to amounts of HBV DNA.

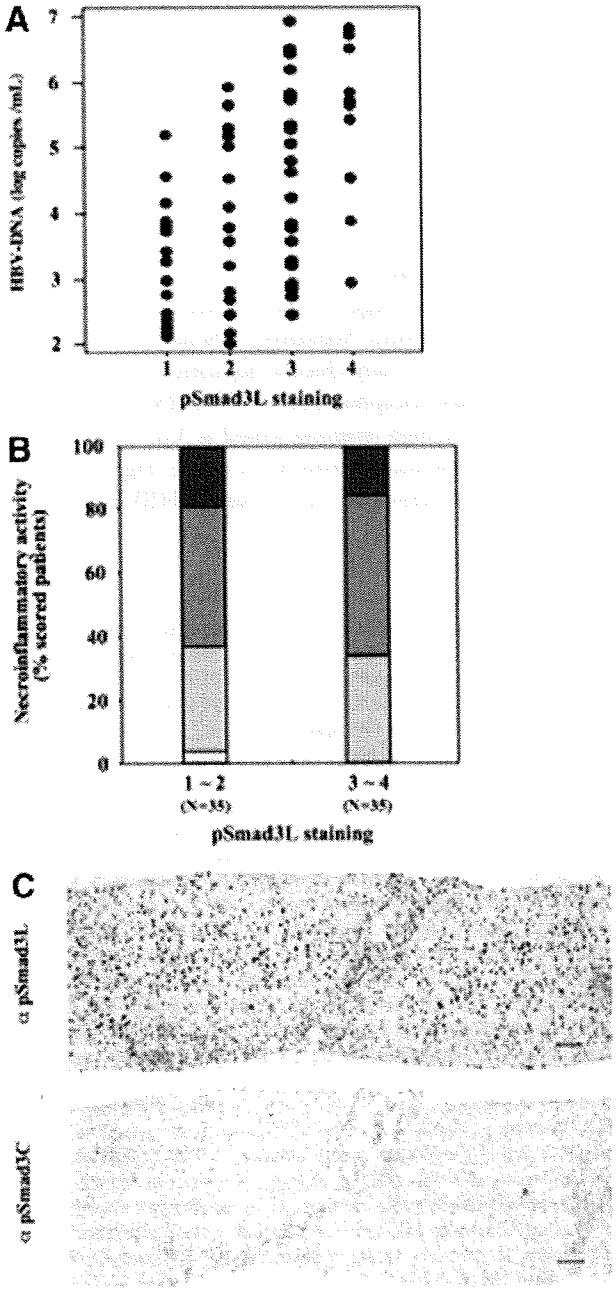

Sixteen sera samples of 35 patients with abundant Smad3L phosphorylation (scores 3 to 4) but only seven sera samples of 35 patients with little Smad3L phosphorylation (scores 0 to 2) contained more than 5.0 log copies/mL (45.7% versus 20.0% [$P = 0.02$]) (Fig. 2A). However, 23 of 35 chronic hepatitis B patients with abundant Smad3L phosphorylation and 22 of 35 patients with little Smad3L phosphorylation showed a high level of inflammatory activity (A 2 to 3) (65.7% versus 62.9% [$P = 0.80$]) (Fig. 2B). These results indicated that HBV itself could up-regulate the hepatocytic phosphorylation at Smad3L, but inflammation could not strongly affect linker phosphorylation.

To further confirm the direct effects of HBV, besides chronic inflammation, on phosphorylation at Smad3L in early chronic hepatitis B, we examined the degrees of pSmad3L and pSmad3C in a group of patients with little fibrosis (F1), little inflammation (A1), and high plasma HBV DNA. Smad3L was highly phosphorylated in hepatocytic nuclei, whereas the phosphorylation at Smad3C was suppressed (Fig. 2C). Of 20 chronic hepatitis B samples, 12 samples showed abundant Smad3L phosphorylation (scores 3 to 4), but only five samples had abundant Smad3C phosphorylation (60.0% versus 25.0% [$P = 0.03$]) (Table 4).

HBx Protein Involvement in c-Myc–Mediated Oncogenic Activity via the pSmad3L Pathway in Human Chronic Hepatitis B. Integrated viral sequences produce HBx protein, which brings about up-regulation of c-Myc oncoprotein.[25] We therefore investigated whether HBx protein affected Smad3L phosphorylation and expression of c-Myc in biopsy specimens from HBV-infected livers by immunostaining sections for

Fig. 2. In proportion to plasma HBV DNA levels, JNK-dependent pSmad3L became prominent in the nuclei of hepatocytes in human early chronic hepatitis B. (A) Positivity for pSmad3L in hepatocytic nuclei in chronic hepatitis B specimens was greater in proportion to plasma HBV DNA levels. Patients with strong pSmad3L positivity in hepatocytic nuclei (staining scored as 3 or 4) had more HBV DNA in plasma than patients with weak pSmad3L positivity (staining scored as 0 to 2). Hepatocytic Smad3 phosphorylation in chronic hepatitis B specimens is scored as follows: 0, no phosphorylation; 1, <25%; 2, 25% to 50%; 3, 50% to 75%; 4, >75%. (B) Degree of Smad3 phosphorylation at the linker region did not strongly correlate with necroinflammatory activity of chronic hepatitis B. Hepatocytic Smad3 phosphorylation at the linker region in livers with necroinflammatory activities of A2 to A3 was essentially similar to phosphorylation in those with activities of A0 to A1. Extent of necroinflammatory activity: □, 0; □, 1; ▒, 2; ■, 3. (C) Smad3 in the nuclei of hepatocytes was phosphorylated intensely at linker region (α pSmad3L column) but sparsely at the C-terminal region (α pSmad3C column). The liver specimen showing minimal fibrosis (F1) and inflammation (A1) was obtained from patient 10 in Table 2 who showed high plasma HBV DNA and was diagnosed with HCC 4 years later.

Table 4. Clinicopathologic Features, Smad3L/C Phosphorylation, and Plasma HBV DNA Levels in Specimens from Patients with Early Chronic Hepatitis B

Patient No.	Sex	Age	pSmad3L staining*	pSmad3C staining*	Fibrotic Stage†	Inflammatory Activity†	HBV DNA (log copies/mL)
1	M	46	4	2	1	1	5.6
2	M	45	4	2	1	1	5.4
3	F	38	3	1	1	1	6.2
4	F	49	3	1	1	1	5.2
5	F	52	3	1	1	1	6.1
6	F	40	3	2	1	1	5.8
7	F	28	3	2	1	1	5.6
8	M	38	3	2	1	1	5.5
9	M	44	3	2	1	1	5.3
10	F	40	3	2	1	1	5.4
11	M	55	3	2	1	1	5.1
12	F	43	3	3	1	1	5.8
13	M	34	2	1	1	1	5.2
14	M	28	1	1	1	1	5.2
15	F	35	1	2	1	1	5.1
16	M	30	1	2	1	1	5.3
17	M	45	1	3	1	1	5.2
18	M	38	1	4	1	1	5.6
19	M	54	1	4	1	1	5.2
20	M	48	1	4	1	1	5.4

Abbreviations: F, female; HBV, hepatitis B virus; M, male; pSmad3C, C-terminally phosphorylated Smad3; pSmad3L, linker-phosphorylated Smad3.

*Hepatocytic Smad3 phosphorylation is scored as follows: 0, no phosphorylation; 1, <25% Smad3 phosphorylation; 2, 25% to 50% Smad3 phosphorylation; 3, 50% to 75% Smad3 phosphorylation; 4, >75% Smad3 phosphorylation.

†Necroinflammatory activity and fibrotic stage are determined histologically according to Desmet's classification.

pSmad3L, paired with sections immunostained for HBx and c-Myc.

In specimens from patient 3 in Table 2 with chronic hepatitis B, pSmad3L, HBx, and c-Myc were distributed in hepatocytes throughout liver lobules (Fig. 3A and Supplementary Fig. 2). Double immunofluorescence studies in chronic hepatitis B specimens confirmed that pSmad3L was colocalized in HBx- and c-Myc–immunoreactive hepatocytes (Fig. 3B). HBx and c-Myc expression increased in hepatocytes of hepatitis B specimens as Smad3 showed more phosphorylation at the linker region (Fig. 3C).

Increased JNK/pSmad3L/c-Myc Oncogenic Signaling and Impaired pSmad3C/p21 ^{WAF1} Tumor-Suppressive Signaling as Chronic Hepatitis B Progresses From Cirrhosis to HCC. We further investigated tumor-suppressive and oncogenic Smad3 signaling in biopsy specimens during HBV-related hepatocarcinogenesis by staining sections using anti-pSmad3L Ab and anti-pSmad3C Ab, paired with sections stained for anti–c-Myc Ab and anti-p21^{WAF1} Ab. Although pSmad3L accelerates tumor growth by up-regulating c-Myc, pSmad3C participates in tumor suppression by up-regulating p21^{WAF1} transcription.[16,20]

In specimens from a patient with chronic hepatitis B, the distribution of pSmad3L fit well with the pattern shown by c-Myc immunolabeling (Fig. 4A, chronic hepatitis panel): both were strong in hepatocytes throughout liver lobules. Linker phosphorylation and c-Myc staining increased further as chronic liver disease progressed through cirrhosis to HCC (Fig. 4A, cirrhosis and HCC panels).

Distribution of pSmad3C resembled the pattern obtained by p21^{WAF1} staining in chronic hepatitis B specimens (Fig. 4B, chronic hepatitis panel). As with pSmad3C distribution, hepatocytes showed increased p21^{WAF1} staining in nuclei. In contrast to intense staining for pSmad3L and c-Myc, pSmad3C and p21^{WAF1} staining decreased in hepatocytic nuclei in cirrhotic liver (Fig. 4B, cirrhosis panel). Nuclear pSmad3C and p21^{WAF1} immunostaining showed only a scattered distribution throughout HCC specimens (Fig. 4B, HCC panel). Semiquantitative analyses of positivity for pSmad3L, pSmad3C, and c-Myc in HBV-related chronic liver disease showed increasing pSmad3L/c-Myc and decreasing pSmad3C as chronic hepatitis B progressed from cirrhosis (F4) to HCC (Table 1).

We next quantified the extent of phosphorylation at Smad3L and Smad3C by immunoblotting with domain-specific Abs against phosphorylated Smad3 in tissue samples representing various stages of HBV-related chronic liver disorders. The linker region of Smad3 showed very little phosphorylation in normal liver (Fig. 4C, α pSmad3L panel). Remarkable up-

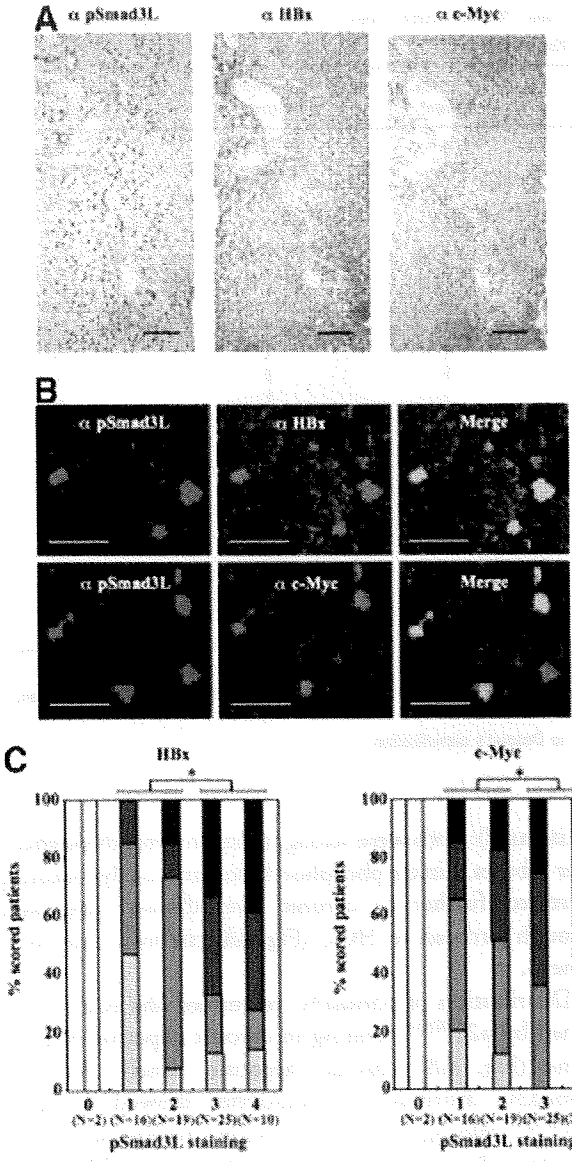

Fig. 3. HBx might be involved in c-Myc-mediated oncogenic activity in human chronic hepatitis B via the pSmad3L pathway. (A) Hepatocytes of chronic hepatitis B specimens from patient 3 in Table 2 showed diffuse immunostaining for pSmad3L, HBx, and c-Myc. All sections were counterstained with hemotoxylin (blue). Brown color indicates specific Ab reactivity. Bar = 50 μm. (B) pSmad3L in hepatocytic nuclei of chronic hepatitis B specimens was colocalized with HBx and c-Myc proteins. Sections of chronic hepatitis B tissues were stained for immunofluorescence to simultaneously detect pSmad3L (red) and HBx or c-Myc (green). Yellow color indicates overlap of proteins. Hepatocytes immunoreactive for pSmad3L showed colocalization of HBx (upper column) and c-Myc (lower column). Bar = 50 μm. (C) HBx and c-Myc expression increased in hepatocytes of chronic hepatitis B specimens as Smad3 was increasingly phosphorylated at the linker region. HBx and c-Myc expression was greater in hepatocytes with high phosphorylation at Smad3L (staining scored as 3 or 4) than in hepatocytes with staining scored as 0 to 2. The extent of HBx and c-Myc expression is indicated as that of pSmad3L positivity: □, 0; □, 1; ▒, 2; ▒, 3; ■, 4. *$P < 0.05$.

regulation of pSmad3L was seen with progression of hepatic fibrosis and carcinogenesis. In cirrhotic liver and HCC, pSmad3L was far more abundant than in chronic hepatitis. In contrast, pSmad3C gradually decreased as disease stages progressed toward HCC (Fig. 4C, α pSmad3C panel).

We previously reported that Smad3L served as a substrate for JNK.[12] To address the functional relationship between activated JNK and Smad3L phosphorylation during hepatocarcinogenesis, we presently assayed kinase activity *in vitro*. Although JNK from normal liver showed little ability to phosphorylate Smad3 at the linker region, JNK from livers involved by chronic hepatitis B, cirrhosis, and HCC could directly phosphorylate Smad3L (Fig. 4D). These results suggested that JNK in preneoplastic liver tissues and HCC directly phosphorylated the linker region of Smad3.

Collectively, JNK/pSmad3L/c-Myc onogenic signaling in hepatocytes came to predominate while the tumor-suppressive pSmad3C/$p21^{WAF1}$ pathway became quiescent as chronic hepatitis B progressed to cirrhosis and then HCC.

Selective Blockade of Linker Phosphorylation Abolishes pSmad3L-Mediated Cell Growth in HBx-Expressing Hepatocytes. pSmad3L, HBx, and c-Myc were colocalized in preneoplastic lesions including chronic hepatitis and cirrhosis (Fig. 3). These findings suggest that HBx oncoprotein might alter hepatocytic TGF-β signaling in chronic hepatitis B. We investigated this hypothesis using HBx-expressing hepatocytes. Selective blockade of linker phosphorylation by a mutant Smad3 lacking the JNK-dependent linker phosphorylation sites abolished pSmad3L-mediated cell growth in HBx-expressing hepatocytes (Supplementary Figs. 3-5). These results suggest that HBx activated the JNK/pSmad3L pathway, further promoting cell proliferation by up-regulating c-Myc transcription (Fig. 5).

Activation of the pSmad3L/c-Myc Pathway as HBx Transgenic Mouse Livers Progress Through Hyperplasia to HCC. We further investigated localization of pSmad3L, HBx, and c-Myc during HBx-induced hepatocarcinogenesis in HBx transgenic mouse livers. Beginning at the age of 2 months, HBx transgenic mouse liver showed centrilobular foci of cellular alteration with cytoplasmic vacuolation surrounding the central veins where bromodeoxyuridine was uptaken into the hepatocytes.[6]

In this hyperplastic mouse liver, phosphorylation at Smad3L was observed in hepatocytic nuclei in the centrilobular region, and distribution of pSmad3L was similar to those of HBx and c-Myc (Fig. 6A). pSmad3L, HBx,

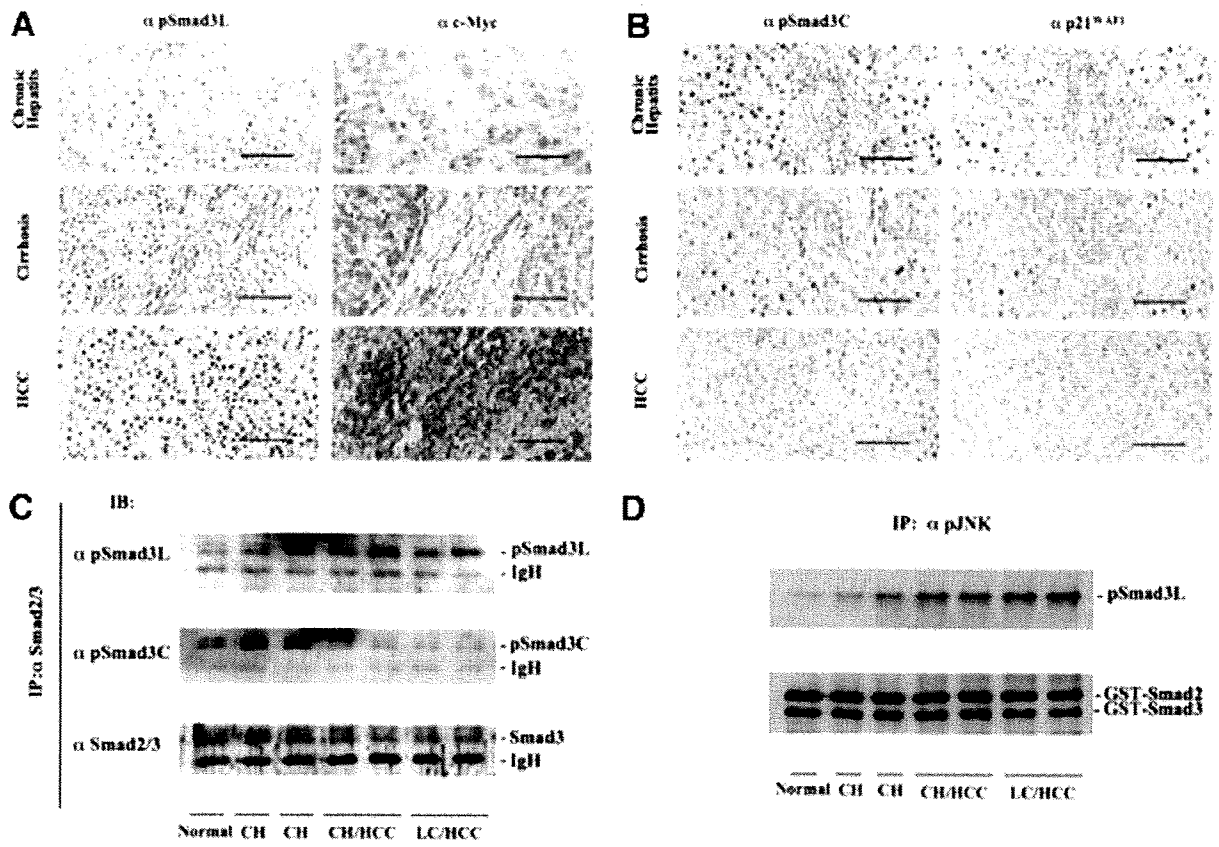

Fig. 4. As chronic hepatitis B progressed through cirrhosis to HCC, JNK/pSmad3L/c-Myc ongogenic signaling started to increase, whereas the tumor-suppressive pSmad3C/p21^{WAF1} pathway decreased. (A) pSmad3L and c-Myc increased as human chronic hepatitis B progressed through cirrhosis to HCC. (B) pSmad3C and p21^{WAF1} decreased as human chronic hepatitis B progressed through cirrhosis to HCC. All sections in A and B were counterstained with hemotoxylin (blue). Brown staining indicates specific Ab reactivity. Bar = 50 μm. (C) Immunoblotting of pSmad3L and pSmad3C in HBV-related chronic liver diseases. Cell lysates obtained from hepatocellular carcinoma (HCC) and surrounding nonneoplastic liver tissues including chronic hepatitis B (CH) or liver cirrhosis (LC) as well as uninvolved normal liver tissues from a patient with a metastatic liver tumor were subjected to anti-Smad3 immunoprecipitation (IP) and were then immunoblotted with each anti-pSmad3 Ab (upper panels). Relative amounts of endogenous Smad3 were determined via immunoblotting using anti-Smad3 Ab (bottom panel). (D) JNK in human HBV-related chronic liver tissue directly phosphorylated Smad3 at the linker region. Cell lysates obtained from HCC and surrounding nonneoplastic liver tissue including chronic hepatitis (CH) and liver cirrhosis (LC) from HBV-infected patients, as well as uninvolved normal liver tissue from a patient with a liver metastasis, were subjected to anti-phospho-JNK1/2 immunoprecipitation (IP), and were then mixed with bacterially expressed GST-Smad3 and GST-Smad2. After *in vitro* kinase assay, phosphorylation of Smad3L was analyzed via immunoblotting using anti-pSmad3L antibody (upper panel). Total Smad3 and Smad2 were determined via immunoblotting using anti-Smad2/3 Ab (lower panel).

and c-Myc were distributed diffusely in HCC specimens (Fig. 6B, HCC panel). Semiquantitative analyses of positivity for these molecules in HBx transgenic mouse livers also revealed that hepatocytic pSmad3L, HBx, and c-Myc increased as mouse liver progressed through hyperplasia to HCC (Fig. 6C). Double immunofluorescence studies in hyperplastic specimens confirmed that pSmad3L was colocalized in HBx- and c-Myc-immunoreactive hepatocytes (Fig. 6D).

Success in comparative study of HBx, pSmad3L, and c-Myc positivity during human and mouse hepatocarcinogenesis identified pSmad3L as a key regulatory element that offers a general framework for understanding the origins of HBV-related HCC.

Chronic Hepatitis B Patients with Hepatocytes Positive for pSmad3L and Negative for pSmad3C Increased Risk of HCC Development. We finally investigated whether phosphorylation levels of Smad3 could affect the risk of neoplastic evolution in the patients with chronic hepatitis B (Table 2). To compare HCC incidence, patients were classified into those with abundant (scores 3 to 4) and limited (scores 0 to 2) Smad3 phosphorylation in hepatocytic nuclei. HCC developed in six of 28 patients with abundant Smad3L phosphory-

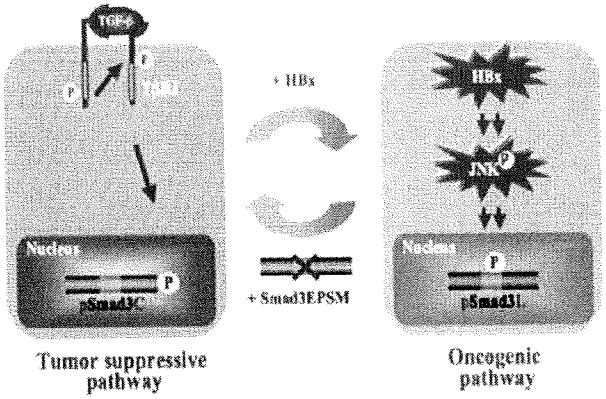

Fig. 5. Reversibility of Smad3-dependent signaling between tumor suppression and oncogenesis in HBx-expressing hepatocytes. Hepatocytes exhibit TGF-β–dependent Smad3 phosphorylation at the C-terminal region, which results in growth inhibition by repression of c-Myc. High expression of HBx protein in hepatocytes tends to shut down pSmad3C-mediated signaling and favor acquisition of constitutively active JNK-mediated pSmad3L signaling, which fosters cell growth by up-regulating c-Myc. Selective blockade of linker phosphorylation by a mutant Smad3 lacking the JNK-dependent linker phosphorylation sites (Smad3EPSM) restores the TGF-β–dependent tumor-suppressive response involving pSmad3C that is shown by parental hepatocytes.

lation, but in only one of 32 patients with limited Smad3L phosphorylation (log-rank = 0.03) (Fig. 7A). In contrast, HCC developed only in the patients with limited Smad3C phosphorylation, and no patients with abundant hepatocytic pSmad3C developed HCC (log-rank = 0.009) (Fig. 7B).

Several studies have analyzed risk factors for HCC occurrence in patients with HBV-related chronic liver disease, including elevated plasma HBV DNA[24] and seropositivity for hepatitis B e antigen.[26] In the univariate analysis, HCC occurrence in high pSmad3L positivity ($P = 0.01$), low pSmad3C positivity ($P = 0.03$), and plasma HBV-DNA levels of more than 5.0 log copies/mL ($P = 0.05$) showed P values less than 0.10, thus being significantly associated with HCC (Table 5). All variables with statistical significance in the univariate analysis were entered in the multivariate analysis, and high pSmad3L and low pSmad3C positivity were considered significantly predictive of HCC development within 12 years. Hepatocytic positivitiy for pSmad3L and pSmad3C should allow us to distinguish chronic hepatitis B patients at high and low risk for the development of HCC in near future.

Discussion

In patients with chronic hepatitis B, persistent HBV infection is clearly the primary inducer of HCC.[1-7] Comparative studies that seek to identify conserved oncogenic signaling common to HCC in both humans and experimental animals will help to eventually identify the molecular pathways that drive the development of HCC.[27] Much is known about the morphologic changes of cells and tissues that precede and accompany development of HCC in humans, allowing earlier diagnosis in some instances.[28] A variety of molecular alterations have been detected in fully developed HCC and to a lesser extent in morphologically defined preneoplastic precursor lesions.[29] Our current studies compared pSmad3L- and pSmad3C-mediated signaling in biopsy specimens of chronic hepatitis, cirrhosis, or HCC from 90 patients with chronic HBV infection versus signaling in preneoplastic and neoplastic liver lesions of HBx transgenic mice. Taken together with the results of *in vitro* experiments using HBx-expressing hepatocytes, our findings indicate that the HBx oncoprotein participates directly in hepatocarcinogenesis by shifting hepatocytic Smad3-mediated signaling from tumor suppression to oncogenesis in patients with early chronic hepatitis B (Fig. 7C). According to the two-step model of carcinogenesis (initiation and promotion), tumor formation can be explained by permanent HBx-dependent activation of the JNK/pSmad3L cascade that has a tumor promoter-like action.

HCC is a human neoplasm associated with viral infection.[1,3] At present, hepatitis virus–associated carcinogenesis can be seen as a multifactorial process that includes both direct and indirect mechanisms.[19] A major factor in the process of HCC development is the host immune system.[30] Chronic inflammation, degeneration, and regeneration induced by the host cellular immune response are common to a variety of human liver diseases, and subsequent cellular proliferation might increase the risk of cancer. We previously reported that increased phosphorylation of Smad3L and decreased phosphorylation of Smad3C were associated with an increased risk of HCV-related HCC.[20] Similarly to HCV-related chronic liver disease, strong pSmad3L positivity was observed in the late stages of HBV-related chronic liver disease (F3 to F4) (Fig. 1C). Considering the development of HCC in HCV core gene-transgenic mice,[31] hepatitis viruses themselves together with the host immune response might promote human hepatocarcinogenesis via the JNK/pSmad3L pathway during the late stage of the carcinogenic process in both HBV- and HCV- related chronic liver disease.

However, HBV and HCV have different roles in human hepatocarcinogenesis when early chronic hepatitis (F1 to F2) is considered. The histological severity of HCV-related liver disease correlates closely with the risk

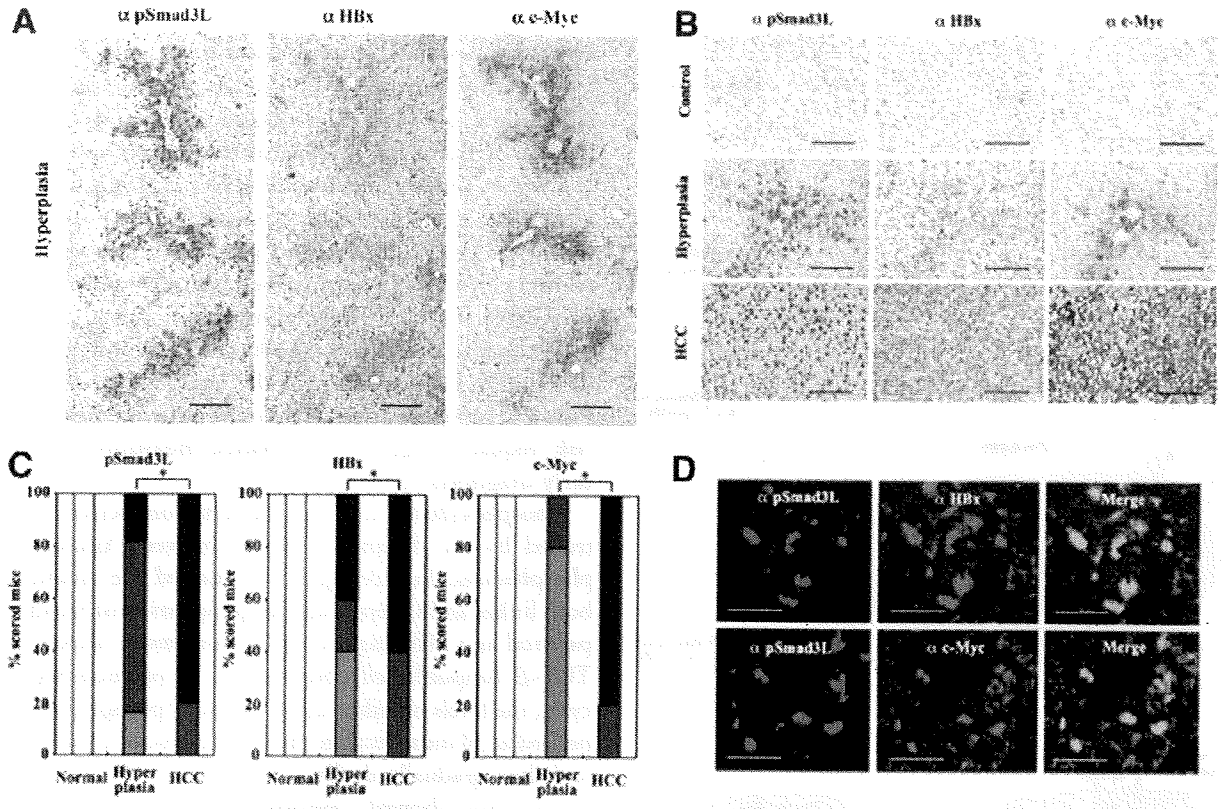

Fig. 6. The pSmad3L/c-Myc pathway was activated as HBx transgenic mouse liver progressed through hyperplasia to HCC. (A) Distribution of pSmad3L, HBx, and c-Myc in hyperplastic specimens from HBx transgenic mouse liver. (B) Distributions of pSmad3L, HBx, and c-Myc in normal liver, hyperplasia, and HCC specimens from HBx transgenic mice. Immunostaining for pSmad3L, HBx, and c-Myc was present in hyperplastic hepatocytes surrounding central veins in HBx transgenic mouse liver [(A) and (B), hyperplasia panels], and was distributed diffusely in HCC specimens [(B), HCC panel]. All sections were counterstained with hemotoxylin (blue). Brown color indicates specific Ab reactivity. Bar = 50 μm. (C) Hepatocytic pSmad3L, HBx, and c-Myc increased as HBx transgenic mouse liver progressed from hyperplasia to HCC. Staining for pSmad3L, HBx, and c-Myc was detected minimally in normal mouse livers, but was strongly up-regulated in neoplastic livers. In HCC, pSmad3L, HBx, and c-Myc were significantly greater than in livers with hyperplasia. $^*P < 0.05$. Extent of pSmad3L, HBx, and c-Myc: □, 0; ▯, 1; ▯, 2; ▩, 3; ■, 4. (D) Hepatocytic pSmad3L in hyperplastic specimens from HBx transgenic mouse liver was colocalized with HBx and c-Myc. Hyperplasia sections of HBx transgenic mouse livers were stained for immunofluorescence to simultaneously detect pSmad3L (red) and HBx or c-Myc (green). Yellow color indicates overlap of proteins. Hepatocytes immunoreactive for pSmad3L showed colocalization of HBx (upper column) and c-Myc (lower column). Bar = 50 μm.

of HCC.[32] In contrast, HCC occasionally develops in healthy HBV surface antigen carriers, who are persistently infected with HBV but have normal liver function parameters and no necroinflammation.[33] This indicates that HBV itself has a direct influence on hepatocarcinogenesis in early chronic hepatitis B. Although integration of the viral genome into chromosomal DNA has not been reported in patients with HCV infection, integration of HBV has been detected in almost all cases of chronic hepatitis B,[3] leading to activation of the HBx-mediated oncogenic pathway.[4] It is noteworthy that HCC developed in patient 10 (Table 2), who showed strong pSmad3L positivity of hepatocytic nuclei but had minimal necroinflammatory activity (A1) or fibrosis (F1). In summary, HCV contributes indirectly to the development of HCC through chronic inflammation in early chronic hepatitis C. In contrast, HBV directly triggers the JNK/pSmad3L oncogenic pathway in early chronic hepatitis B, thus playing a role beyond mere stimulation of the host immune response.

Our findings also open up a new avenue to understanding the development and progression of hepatic fibrogenesis.[34] Whereas HSCs have traditionally been considered as the principal source of liver fibrosis, mature hepatocytes can acquire a mesencymal phenotype and perform the functions of activated HSC—that is, they can contribute to fibrogenesis.[35,36] In support of this notion, pSmad3L-mediated signaling promotes liver fibrosis by hepatocytes as well as activated HSCs during long-standing carcinogenesis.[13,18,20] In this manner, either HBV- or HCV-related chronic hepatitis progresses through fibrogenesis to HCC.

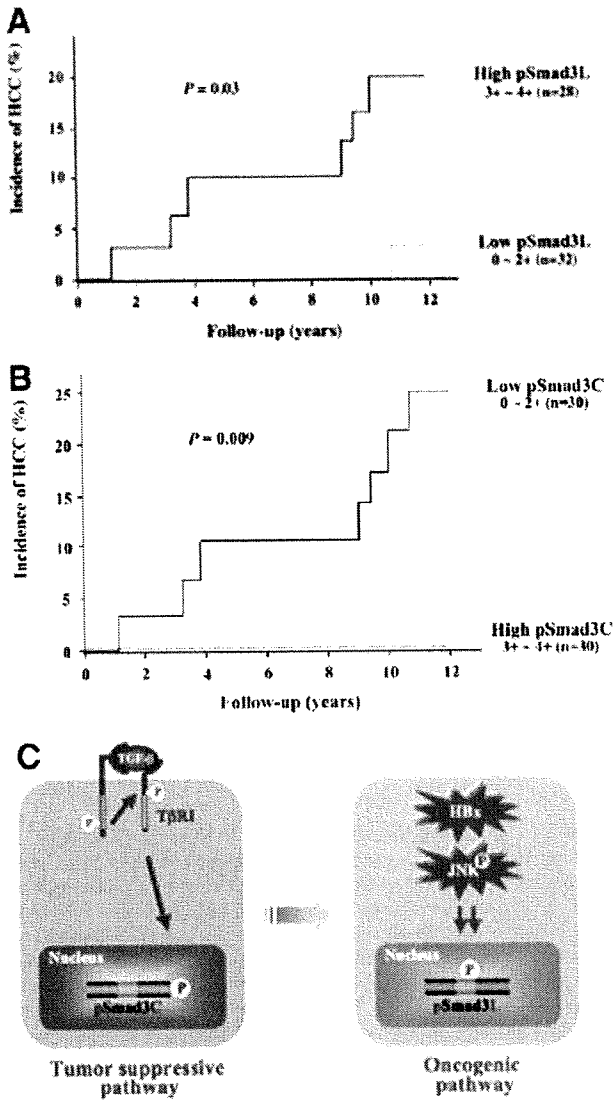

Fig. 7. Chronic hepatitis B patients with hepatocytes positive for pSmad3L and negative for pSmad3C increased risk of HCC development. (A) HCC occurred subsequently among patients whose hepatocytes in chronic hepatitis B specimens were strongly positive for pSmad3L. Incidence of HCC was significantly higher in patients with abundant Smad3L phosphorylation (scores 3 to 4, solid line) in hepatocytic nuclei versus those with sparse Smad3L phosphorylation (scores 0 to 2, dotted line). (B) HCC did not occur subsequently among patients whose hepatocytes in chronic hepatitis B specimens were strongly positive for pSmad3C. HCC occurred only in patients with sparse Smad3C phosphorylation (scores 0 to 2, solid line) in hepatocytic nuclei, while no patients with abundant Smad3C phosphorylation (scores 3 to 4, dotted line) have developed HCC. Cumulative rates of HCC occurrence from chronic hepatitis B were compared between cases with high and low phosphorylation of Smad3L and Smad3C (Kaplan-Meier analysis and log-rank test). (C) HBx protein shifted hepatic TGF-β signaling from the tumor-suppressive pSmad3C pathway to the oncogenic JNK-dependent pSmad3L pathway in early stages of chronic hepatitis B. Normal hepatocytes exhibited TGF-β-dependent Smad3 phosphorylation at the C-terminal region, which is related to growth inhibition by up-regulation of $p21^{WAF1}$. HBx protein activates JNK, promoting the oncogenic pSmad3L signaling, which fosters cell growth by up-regulating c-Myc, in a mean time reducing tumor-suppressive pSmad3C-mediated signaling.

The general biomedical approach to HCC is shifting away from population risk assessment and empirical treatment of patients to predictive personalized medicine based on molecular classification and targeted therapy.[29] Better knowledge of the risk factors associated with the occurrence of HCC can improve the effectiveness of surveillance programs. Our approach has identified pSmad3L and pSmad3C as prognostic markers that may prove to be clinically useful. Such predictive markers could allow us to select patients with chronic hepatitis B who have a high or low risk of developing HCC. Although the latter group could be followed up on an annual basis, the patients with a high risk require targeted surveillance measures to allow early diagnosis of HCC.

Phosphorylation of many transcription factors is controlled by the dynamic interplay between kinases and phosphatases. In this regard, we studied the kinetics of both linker and C-terminal phosphorylation of Smad3 in parental and HBx-expressing hepatocytes in response to TGF-β (unpublished observation). In parental hepatocytes, the levels of linker and C-terminal phosphorylation peaked at 30 minutes after the start of exposure to TGF-β and then gradually declined. However, HBx-expressing hepatocytes showed constitutive phosphorylation at Smad3L during continuous exposure to TGF-β. Several lines of evidence have identified small C-terminal domain phosphatase (SCP1-3) and protein phosphatase magnesium 1A (PPM1A) as the linker and C-terminal phosphatases, respectively.[37,38] Accordingly, SCP1-3 and PPM1A may reverse domain-specific phosphorylation in normal hepatocyes. In contrast, HBx-expressing hepatocytes may not show induction or activation of SCP1-3. Alternatively, linker phosphorylation in HBx-expressing hepatocytes might be resistant to SCP1-3.

Many researchers have been seeking key transcription factors regulating tumor-suppressive pathways that are altered in cancer. Our current model of JNK/pSmad3L signaling during HBV-related chronic liver disease suggests that specific inhibitors of the JNK/pSmad3L pathway might inhibit the progression of HCC. With respect to molecular targeting therapy for human HCC, pSmad3L and pSmad3C should be assessed as biomarkers to evaluate the benefit from specific inhibition of the JNK/pSmad3L pathway.

Acknowledgment: We thank Dr. Rik Derynck (University of California at San Francisco) and Dr. Seishi Murakami (Kanazawa University) for providing us with complementary DNAs encoding human Smad3 and HBx. We also thank Chiaki Kitano for assistance to construct ecotropic retrovirus and Natsuko Ohira for assistance with immunoblotting.

Table 5. Variables with Independent Predictive Value for HCC in Univariate and Multivariate Analyses

Characteristics	n	No. of Patients with HCC (%)	Univariate Analysis		Multivariate Analysis	
			Hazard Ratio (95% CI)	P Value	Hazard Ratio (95% CI)	P Value
pSmad3L positivity*						
Low (1 and 2)	32	1 (3)	1.00		1.00	
High (3 and 4)	28	6 (21)	3.8 (1.4-10.6)	0.01	14.8 (1.8-118.5)	0.01
pSmad3C positivity*						
High (3 and 4)	30	0 (0)	1.00		1.00	
Low (1 and 2)	30	7 (23)	2.8 (0.001-7.0)	0.03	16.4 (1.0-125.0)	0.04
Fibrotic stage†						
Low (F1 and F2)	39	4 (10)	1.00		1.00	
High (F3)	21	3 (14)	1.9 (0.7-5.4)	0.24	3.9 (0.4-38.6)	0.24
Inflammatory activity†						
Low (A0 and A1)	23	1 (4)	1.00		1.00	
High (A2 and A3)	37	6 (16)	1.8 (0.7-4.8)	0.27	0.2 (0.02-1.1)	0.06
HBV DNA (copies /mL)						
$<10^5$	42	3 (7)	1.00		1.00	
$>10^5$	18	4 (22)	1.9 (1.0-3.5)	0.05	2.5 (0.9-6.9)	0.08
HBeAg						
Negative	42	4 (10)	1.00		1.00	
Positive	18	3 (17)	2.1 (0.5-9.5)	0.32	9.9 (1.1-89.3)	0.03

Abbreviations: CI, confidence interval; HBeAg, hepatitis B e antigen; HBV, hepatitis B virus; HCC, hepatocellular carcinoma; pSmad3C, C-terminally phosphorylated Smad3; pSmad3L, linker-phosphorylated Smad3.

*Hepatocytic Smad3 phosphorylation in chronic hepatitis B specimens is scored as follows: 0, no phosphorylation; 1, <25% Smad3 phosphorylation; 2, 25% to 50% Smad3 phosphorylation; 3, 50% to 75% Smad3 phosphorylation; 4, >75% Smad3 phosphorylation.

†Necroinflammatory activity and fibrotic stage are determined histologically according to Desmet's classification.

References

1. Llovet JM, Burroughs A, Bruix J. Hepatocellular carcinoma. Lancet 2003; 362:1907-1917.
2. El-Serag HB. Hepatocellular carcinoma: recent trends in the United States. Gastroenterology 2004;127(Suppl):27S–34S.
3. Brechot C, Pourcel C, Louise A, Rain B, Tiollais P. Presence of integrated hepatitis B virus DNA sequences in cellular DNA of human hepatocellular carcinoma. Nature 1980;286:533-535.
4. Kim CM, Koike K, Saito I, Miyamura T, Jay G. HBx gene of hepatitis B virus induces liver cancer in transgenic mice. Nature 1991;351:317-320.
5. Yu DY, Moon HB, Son JK, Jeong S, Yu SL, Yoon H, et al. Incidence of hepatocellular carcinoma in transgenic mice expressing the hepatitis B virus X-protein. J Hepatol 1999;31:123-132.
6. Koike K, Moriya K, Iino S, Yotsuyanagi H, Endo Y, Miyamura T, et al. High-level expression of hepatitis B virus HBx gene and hepatocarcinogenesis in transgenic mice. HEPATOLOGY 1994;19:810-819.
7. Benn J, Su F, Doria M, Schneider RJ. Heptitis B virus HBx protein induces transcription factor AP-1 by activation of extracellular signal-related and c-Jun N-terminal mitogen-activated protein kinases. J Virol 1996;70: 4978-4985.
8. Roberts AB, Sporn MB. The transforming growth factor-βs. In: Sporn MB, Roberts AB, eds. Peptide Growth Factors and Their Receptors. Berlin: Springer-Verlag, 1990:419-472.
9. Heldin CH, Miyazono K, ten Dijke P. TGF-β signaling from cell membrane to nucleus through SMAD proteins. Nature 1997;390:465-471.
10. Massagué J. TGF-β signal transduction. Annu Rev Biochem 1998;67: 753-791.
11. Kretzschmar M, Doody J, Timokhina I, Massague J. A mechanism of repression of TGF-β/Smad signaling by oncogenic Ras. Genes Dev 1999; 13:804-816.
12. Mori S, Matsuzaki K, Yoshida K, Furukawa F, Tahashi Y, Yamagata H, et al. TGF-β and HGF transmit the signals through JNK-dependent Smad2/3 phosphorylation at the linker regions. Oncogene 2004;23:7416-7429.
13. Furukawa F, Matsuzaki K, Mori S, Tahashi Y, Yoshida K, Sugano Y, et al. p38 MAPK mediates fibrogenic signal through Smad3 phosphorylation in rat myofibroblasts. HEPATOLOGY 2003;38:879-889.
14. Matsuura I, Denissova NG, Wang G, He D, Long J, Liu F. Cyclin-dependent kinases regulate the antiproliferative function of Smads. Nature 2004;430:226-231.
15. Yamagata H, Matsuzaki K, Mori S, Yoshida K, Tahashi Y, Furukawa F, et al. Acceleration of Smad2 and Smad3 phosphorylation via c-Jun NH(2)-terminal kinase during human colorectal carcinogenesis. Cancer Res 2005; 65:157-165.
16. Sekimoto G, Matsuzaki K, Yoshida K, Mori S, Murata M, Seki T, et al. Reversible Smad-dependent signaling between tumor suppression and oncogenesis. Cancer Res 2007;67:5090-5096.
17. Arany PR, Rane SG, Roberts AB. Smad3 deficiency inhibits v-ras-induced transformation by suppression of JNK MAPK signaling and increased farnesyl transferase inhibition. Oncogene 2008;27:2507-2512.
18. Yoshida K, Matsuzaki K, Mori S, Tahashi Y, Yamagata H, Furulawa F, et al. Transforming growth factor-β and platelet-derived growth factor signal via c-Jun N-terminal kinase-dependent Smad2/3 phosphorylation in rat hepatic stellate cells after acute liver injury. Am J Pathol 2005;166:1029-1039.
19. Block TM, Mehta AS, Fimmel CJ, Jordan R. Molecular viral oncology of hepatocellular carcinoma. Oncogene 2003;22:5093-5107.
20. Matsuzaki K, Murata M, Yoshida K, Sekimoto G, Uemura Y, Sakaida N, et al. Chronic inflammation associated with hepatitis C viral infection perturbs hepatic TGF-β signaling, promoting cirrhosis and hepatocellular carcinoma. HEPATOLOGY 2007;46:48-57.
21. Desmet VJ, Gerber M, Hoofnagle JH, Manns M, Scheuer PJ. Classification of chronic hepatitis: diagnosis, grading and staging. HEPATOLOGY 1994;19:1513-1520.
22. Cox DR. Regression models and life-tables. J R Stat Soc (B) 1972;34:187-220.
23. Pardali K, Moustakas A. Actions of TGF-β as tumor suppressor and pro-metastatic factor in human cancer. Biochim Biophys Acta 2007;1775:21-62.

24. Chen CJ, Yang HI, Su J, Jen CL, You SL, Lu SN, et al. REVEAL-HBV study group. Risk of hepatocellular carcinoma across a biological gradient of serum hepatitis B virus DNA level. JAMA 2006;295:65-73.
25. Feitelson MA. c-Myc overexpression in hepatocarcinogenesis. Human Pathology 2004;35:1299-1302.
26. Yang HI, Lu SN, Liaw YF, You SL, Sun CA, Wang LY, et al. Taiwan community-based cancer screening project group. Hepatitis B e antigen and the risk of hepatocellular carcinoma. N Engl J Med 2002;347:168-174.
27. Thorgeirsson SS, Lee JS, Grisham JW. Functional genomics of hepatocellular carcinoma. HEPATOLOGY 2006;43:145-150.
28. Theise ND, Park YN, Kojiro M. Dysplastic nodules and hepatocarcinogenesis. Clin Liver Dis 2002;6:497-512.
29. Thorgeirsson SS, Grisham JW. Molecular pathogenesis of human hepatocellular carcinoma. Nat Genet 2002;31:339-346.
30. Chisari FV, Klopchin K, Moriyama T, Pasquinelli C, Dunsford HA, Sell S, et al. Molecular pathogenesis of hepatocellular carcinoma in hepatitis B virus transgenic mice. Cell 1989;59:1145-1156.
31. Moriya K, Fujie H, Shintani Y, Yotsuyanagi H, Tsutsumi T, Ishibashi K, et al. The core protein of hepatitis C virus induces hepatocellular carcinoma in transgenic mice. Nat Med 1998;4:1065-1067.
32. Di Bisceglie AM. Hepatitis C and hepatocellular carcinoma. HEPATOLOGY 1997;26 (Suppl):34S–38S.
33. Popper H, Shafritz DA, Hoofnagle JH. Relation of the hepatitis B virus carrier state to hepatocellular carcinoma. HEPATOLOGY 1987;7:764-772.
34. Inagaki Y, Okazaki I. Emerging insights into transforming growth factor β Smad signal in hepatic fibrogenesis. Gut 2007;56:284-292.
35. Kaimori A, Potter J, Kaimori JY, Wang C, Mezey E, Koteish A. Transforming growth factor-β1 induces an epithelial-to-mesenchymal transition state in mouse hepatocytes in vitro. J Biol Chem 2007;282:22089-22101.
36. Weng HL, Ciuclan L, Liu Y, Hamzavi J, Godoy P, Gaitantzi H, et al. Profibrogenic transforming growth factor-β/activin receptor-like kinase 5 signaling via connective tissue growth factor expression in hepatocytes. HEPATOLOGY 2007;46:1257-1270.
37. Lin X, Duan X, Liang YY, Su Y, Wrighton KH, Long J, et al. PPM1A functions as a Smad phosphatase to terminate TGFβ signaling. Cell 2006; 125:915-928.
38. Wrighton KH, Willis D, Long J, Liu F, Lin X, Feng XH. Small C-terminal domain phosphatases dephosphorylate the regulatory linker regions of Smad2 and Smad3 to enhance transforming growth factor-β signaling. J Biol Chem 2006;281:38365-38375.

Proteomics Analysis of Mitochondrial Proteins Reveals Overexpression of a Mitochondrial Protein Chaperon, Prohibitin, in Cells Expressing Hepatitis C Virus Core Protein

Takeya Tsutsumi,[1] Mami Matsuda,[2] Hideki Aizaki,[2] Kyoji Moriya,[1] Hideyuki Miyoshi,[1] Hajime Fujie,[1] Yoshizumi Shintani,[1] Hiroshi Yotsuyanagi,[1] Tatsuo Miyamura,[2] Tetsuro Suzuki,[2] and Kazuhiko Koike[1]

The hepatitis C virus (HCV) core protein is involved in viral pathogenesis such as oxidative stress induction and lipid metabolism disturbance, and is primarily located in the cytoplasm and endoplasmic reticulum in association with lipid droplets as well as in the mitochondria. To clarify the impact of the core protein on mitochondria, we analyzed the expression pattern of mitochondrial proteins in core protein-expressing cells by two-dimensional polyacrylamide gel electrophoresis. Several proteins related to the mitochondrial respiratory chain or protein chaperons were identified by mass spectrometry. Among the identified proteins with consistently different expressions, prohibitin, a mitochondrial protein chaperon, was up-regulated not only in core-expressing cells but also in full-genomic replicon cells and livers of core-gene transgenic mice. The stability of prohibitin was increased through interaction with the core protein. Further analysis demonstrated that interaction of prohibitin with mitochondrial DNA-encoded subunits of cytochrome c oxidase (COX) was disturbed by the core protein, resulting in a significant decrease in COX activity. *Conclusion:* The HCV core protein affects the steady-state levels of a subset of mitochondrial proteins including prohibitin, which may lead to an impaired function of the mitochondrial respiratory chain with the overproduction of oxidative stress. (HEPATOLOGY 2009;50:378-386.)

The hepatitis C virus (HCV) is a causative agent of chronic hepatitis, which often leads to cirrhosis and, eventually, to the development of hepatocellular carcinoma (HCC). However, the mechanism of hepatocarcinogenesis in HCV infection is not yet fully elucidated. The HCV core protein forms the viral nucleocapsid protein and has various properties that modulate cellular processes in numerous ways. The core protein binds to cellular proteins, suppresses or enhances apoptosis, and modulates the transcription of some host genes.[1] In addition, transgenic mice expressing the core protein develop HCC,[2-4] indicating a direct contribution of the core protein to the pathogenesis of hepatitis C.

The core protein is mostly localized to the endoplasmic reticulum (ER), but we and other groups have shown its localization to the mitochondria in cultured cells and transgenic mice.[2,5,6] In addition, the double structure of mitochondrial membranes is disrupted in hepatocytes of core-gene transgenic mice.[2-4] Evidence suggests that the core protein modulates some mitochondrial functions, including fatty acid β-oxidation, the impairment of which may induce lipid abnormalities and hepatic steatosis. In addition, the mitochondrion is an important source of reactive oxygen species (ROS). In livers of transgenic

Abbreviations: 2D-PAGE, two-dimensional polyacrylamide gel electrophoresis; COX, cytochrome c oxidase; ER, endoplasmic reticulum; Ero1, ER protein endoplasmic oxidoreduction-1; HCC, hepatocellular carcinoma; HCV, hepatitis C virus; HSP, heat shock protein; IFN, interferon; MnSOD, manganese superoxide dismutase; NS, nonstructural; OST48, oligosaccharyltransferases-48; PDH, pyruvate dehydrogenase; PDI, protein disulfide isomerase; ROS, reactive oxygen species; TFA, trifluoroacetic acid.

From the [1]Department of Internal Medicine, Graduate School of Medicine, University of Tokyo; [2]Department of Virology II, National Institute of Infectious Diseases, Tokyo, Japan.

Received June 17, 2008; accepted March 20, 2009.

Supported by a grant-in-aid for Scientific Research from the Japan Society for the Promotion of Science, from the Ministry of Health, Labour and Welfare of Japan (Research on Hepatitis), from the Ministry of Education, Culture, Sports, Science and Technology (Priority Area), from The Sankyo Foundation of Life Science, and from The Charitable Trust Araki Memorial Promotion Fund. T.T. is an awardee of the Research Resident Fellowship from the Viral Hepatitis Research Foundation of Japan.

Address reprint requests to: Kazuhiko Koike, M.D., Ph.D., Department of Gastroenterology, Internal Medicine, Graduate School of Medicine, University of Tokyo, 7-3-1 Hongo, Bunkyo-ku, Tokyo 113-8655, Japan. E-mail: kkoike-tky@umin.ac.jp; fax: (81) 3-5800-8799

Published online in Wiley InterScience (www.interscience.wiley.com).

DOI 10.1002/hep.22998

Potential conflict of interest: Nothing to report.

Additional Supporting Information may be found in the online version of this article.

mice harboring the core gene, increased ROS production has been observed.[7-9] A recent study found, by the proteomic profiling of biopsy specimens, that an impairment in key mitochondrial processes, including fatty acid oxidation and oxidative phosphorylation, and in the response to oxidative stress occurs in HCV-infected human liver with advanced fibrosis.[10] Therefore, it is probable that the HCV core protein affects mitochondrial functions because such pathogenesis is observed in both HCV core-transgenic mice and HCV-infected patients.[11-13]

The recent progress in proteomics has opened new avenues for disease-related biomarker discovery. Among proteomics approaches, two-dimensional polyacrylamide gel electrophoresis (2D-PAGE) is a technique for the separation and identification of proteins in a sample by displacement in two dimensions oriented at right angles to one another. This method is generally used as a component of proteomics and is the step used for the isolation of proteins for further characterization by mass spectrometry. 2D-PAGE is particularly useful when comparing two related samples such as healthy and diseased tissue. For example, proteins that are more abundant in diseased tissue may represent novel drug targets or diagnostic markers. In fact, several candidate biomarkers for many human cancers have been identified by this approach.[14] There are, however, tens of thousands of proteins in a cell, differing in abundance over six orders of magnitude. 2D-PAGE is not sensitive enough to detect rare proteins, and hence many proteins are not resolved. Therefore, splitting a sample into different fractions is often necessary to reduce the complexity of protein mixtures prior to 2D-PAGE. For this advantage, Lescuyer et al.[15] performed a 2D-PAGE of human mitochondrial proteins derived from the placenta and identified proteins mainly by peptide mass fingerprinting.

In this study, we performed a 2D-PAGE of mitochondria isolated from HepG2 cells stably expressing the HCV core protein and identified several proteins of different expressions when compared with control HepG2 cells. Among up-regulated proteins in the core-expressing cells, we focused on prohibitin, which functions as a mitochondrial protein chaperon, and found that the core protein interacts with prohibitin and represses the interaction between prohibitin and subunit proteins of cytochrome c oxidase (COX), which may lead to decreases in the expression level of the proteins and in COX activity. These results may explain the pathogenesis of liver disease in HCV infection including ROS induction.

Materials and Methods

Cells and Purification of Mitochondria. Hep39 cells,[16] which stably express the HCV core protein, and control HepG2 cells (Hepswx) were grown in Dulbecco's modified Eagle medium (DMEM) containing 10% fetal bovine serum and 1 mg/mL G418. Mitochondria were purified using Nycodenz (Nycomed Pharma, Zürich, Switzerland) according to the protocols reported by Okado-Matsumoto et al.[17] For transient transfection experiments, HepG2 cells were transfected with a core-expression plasmid using TransIT-LT1 (Mirus Bio, Madison, WI). Huh7 cells harboring HCV genotype 1b full-genomic (RCYM1)[18] or subgenomic replicon (5-15), and livers of 3-month-old core-gene transgenic mice[2] were also used for the analysis.

2D-PAGE. Gel electrophoresis in the first dimension was performed using an immobilized pH gradient gel (Immobiline Dry Strip gel, pH 4-7 linear, 13 cm; GE Healthcare, Uppsala, Sweden). The two-dimensional separation was performed on 12.5%, 14 × 16 cm^2, SDS polyacrylamide gels. After the electrophoresis, gels were silver-stained using a silver staining kit (GE Healthcare) according to the manufacturer's protocols. The stained gels were scanned and electronic images of the gels were analyzed using ImageMaster 2D Elite software (GE Healthcare).

In-Gel Digestion and Matrix-Assisted Laser Desorption Ionization, Time-of-Flight Mass Spectrometry (MALDI-TOF-MS). Protein spots on the gels were excised and a "control" piece was cut from a blank region of the gel and processed in parallel with the sample. In-gel digestion with trypsin was performed as reported.[19] The resulting peptides were concentrated using Zip-Tip C18 (Millipore, Bedford, MA). The peptide mixtures were eluted from Zip-Tip with 75% acetonitrile in 0.1% trifluoroacetic acid (TFA). The matrix (α-cyano-4-hydroxycinnamic acid dissolved in 50% acetonitrile, 0.1% TFA) was deposited on a dried sample target. Then 0.5-μL aliquots of the analyte solution were deposited onto matrix surfaces and the solvent was allowed to evaporate at ambient temperature. The digests were analyzed with a TOF mass spectrometer, PE Biosystems Voyager DE STR MALDI (Foster City, CA).

Database Analysis. For protein identification the measured monoisotopic masses of the peptides were analyzed using MS-Fit provided by UCSF (http://prospector.ucsf.edu/ucsfhtml3.2/msfit.htm).

Immunoblotting and Immunoprecipitation. Purified mitochondria were lysed and sonicated in RIPA buffer, then centrifuged at 16,000 rpm for 10 minutes. Protein concentration was determined using a BCA Protein Assay Reagent Kit (Pierce Biotechnology, Rockford, IL). The samples were separated by sodium dodecyl sulfate (SDS)-PAGE and electrotransferred onto a polyvinylidene fluoride membrane (Immobilon; Millipore, Japan), then blocked with BlockAce (Snow Brand, To-

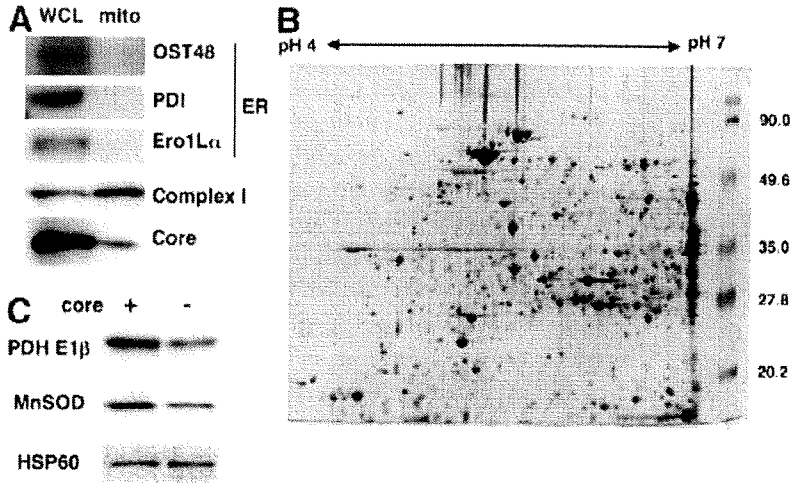

Fig. 1. 2D-PAGE of mitochondria purified from core-expressing cells. (A) Whole-cell lysates (WCL) and purified mitochondria (mito) derived from core-expressing cells were subjected to SDS-PAGE and immunoblotted with anti-core, anti-subunit of complex I (mitochondrial protein), or anti-OST48, PDI, Ero1La (ER proteins) antibodies. (B) Purified mitochondria of core-expressing cells were subjected to 2D-PAGE and the gel was stained with silver. The numbers shown on the right are molecular weights. (C) Purified mitochondria of core-expressing and control cells were subjected to SDS-PAGE and blotted with an anti-E1β subunit of PDH (PDH E1β), anti-MnSOD, or anti-HSP60 antibody.

kyo, Japan). The membrane was subsequently incubated with specific primary antibodies followed by horseradish peroxidase-conjugated secondary antibodies and visualized using SuperSignal West Pico Chemiluminescent Substrate (Pierce). Antibodies against the core protein (Anogen, Mississauga, Canada), manganese superoxide dismutase (MnSOD) (BD Biosciences, San Jose, CA), prohibitin (Neomarkers, Fremont, CA), oligosaccharyltransferase-48 (OST48), heat shock protein (HSP) 60 (Santa-Cruz Biotechnology, Santa Cruz, CA), pyruvate dehydrogenase (PDH), ubiquinol-cytochrome c oxidoreductase, COX (Molecular Probes, Eugene, OR), protein disulfide isomerase (PDI), ER protein endoplasmic oxidoreduction-1 (Ero1)-Lα, and IκBα (Cell Signaling Technology, Danvers, MA), were used as primary antibodies. For immunoprecipitation experiments, cells were lysed in NET-N buffer (20 mM Tris-HCl [pH 8.0], 100 mM NaCl, 1 mM EDTA, 0.5% Nonidet P-40) and the lysates were incubated with anti-prohibitin overnight followed by the addition of protein Sepharose 4B (GE Healthcare), then washed with the same buffer five times. Immunoprecipitates were subjected to SDS-PAGE followed by immunoblotting with specific antibodies.

Determination of COX Activity. COX activity was determined with a MitoProfile Rapid Microplate Assay Kit (MitoSciences, Eugene, OR) using 10 μg of purified mitochondria. The assay was performed three times independently.

Statistical Analysis. Results are expressed as means ± SE. The significance of the difference in means was determined by Student's *t* test or Mann-Whitney's *U* test.

Results

Presence of HCV Core Protein in Purified Mitochondria. Increasing evidence suggests that the HCV core protein is localized to mitochondria as well as to ER and the nucleus. Therefore, we first investigated whether the core protein is expressed in the mitochondria of core-expressing (Hep39) cells used in this study. We used Nycodenz discontinuous gradients to extract mitochondria as described.[17] In the mitochondria derived from core-expressing HepG2 cells, the core protein was detected by immunoblotting, whereas ER resident proteins such as an ER-specific type I transmembrane protein OST48, ER-resident molecular chaperon PDI, and ER membrane-associated N-glycoprotein Ero1-Lα, were not (Fig. 1A). In this fraction, reduced nicotinamide adenine dinucleotide (NADH)-ubiquinone oxidoreductase, complex I of mitochondrial oxidative phosphorylation system, was more strongly expressed than that in the whole cell. These results indicate that the purified mitochondria fraction was free of ER, and that a portion of the core protein was localized to the mitochondria in core-expressing cells.

Proteomics Analysis of Mitochondria by 2D-PAGE. For proteomics analysis, purified mitochondrial proteins derived from core-expressing cells were subjected to 2D-PAGE followed by silver-staining of the gel. In this study we analyzed only acidic proteins using IPG strips covering pH 4 to pH 7 because the analysis of acidic proteins by 2D-PAGE is relatively easy. The mitochondrial fraction was also extracted from Hepswx, a control cell line resistant to G418 but does not express the core protein, then similarly subjected to 2D-PAGE and used for comparing the expression pattern. We repeated the above procedure (purification of mitochondria, 2D-PAGE, and silver-staining) five times, and confirmed a similar expression pattern in core-expressing cells. The representative gel image is shown in Fig. 1B. ImageMaster 2D Elite software detected about 1100 spots on the silver-stained acidic gel, i.e., at pH 4-7 and Mrs of 20-100 kDa. The number of

Table 1. Proteins of Differential Expression in Mitochondria of Core-Expressing Cells

Protein Name	Fold Change (Mean ± SD)
Increased	
Succinyl-CoA:ketoacid CoA transferase	10.43 ± 1.29
NADH-specific isocitrate dehydrogenase a subunit precursor	9.64 ± 4.66
Unknown	8.65 ± 2.40
GrpE-like protein co-chaperon	5.71 ± 0.49
Leucine aminopeptidase	4.26 ± 1.14
Pyruvate dehydrogenase E1 component b subunit	3.79 ± 1.34
CGO15alt2	3.18 ± 0.80
HSP70	3.11 ± 1.39
Prohibitin	2.60 ± 0.24
3-Hydroxyisobutyrate dehydrogenase	2.47 ± 0.77
HSPC108	2.46 ± 0.69
MnSOD	2.35 ± 0.65
Ubiquinol-cytochrome c oxidoreductase core I protein	2.00 ± 0.23
Decreased	
Aldehyde dehydrogenase 2	0.12 ± 0.02
Aldehyde dehydrogenase 5 precursor	0.25 ± 0.03
ATP synthase a subunit isoform 1	0.50 ± 0.09
Reference protein	
HSP60	1.02 ± 0.02

protein spots was smaller than those reported in a recent study investigating the human placental mitochondrial proteome.[15]

We then compared the intensity of the spots between core-expressing and control cells. Analysis of repeated experiments by Student's t test revealed 13 increased and three decreased spots in intensity in core-expressing cells. These spots were excised and digested with trypsin, then proteins were identified by mass spectrometry. The names of the identified proteins are listed in Table 1. Among them were proteins related to mitochondrial respiratory chain, protein chaperons, and lipid metabolism. Because antibodies to some of these proteins are commercially available, expression levels of the proteins were examined by immunoblotting. The expression levels of the PDH-E1β subunit and MnSOD, which were identified as increased proteins, were higher in core-expressing cells than in control cells (Fig. 1C), whereas that of HSP60, which was identified as having a similar expression, was unchanged.

Up-regulation of Prohibitin by the Core Protein. Among the identified proteins, we focused on prohibitin, an up-regulated protein in mitochondria of core-expressing cells (Fig. 2A). Prohibitin is a mitochondrial protein associated with cell proliferation.[20] It also works as a chaperon of mitochondrial proteins.[21,22] We confirmed an increased prohibitin expression level in core-expressing cells

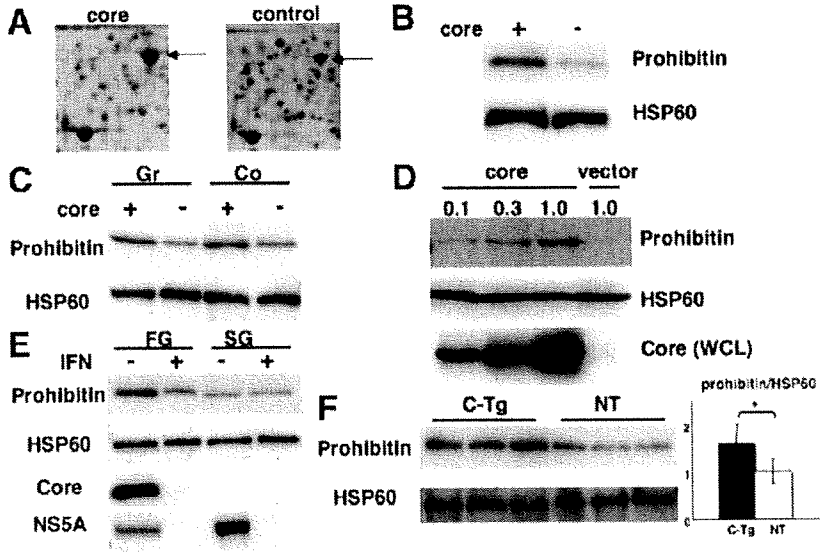

Fig. 2. Up-regulation of prohibitin in core-expressing cells. (A) Protein spot corresponding to prohibitin (arrow) in 2D-PAGE. (B) Purified mitochondria from core-expressing or control cells were subjected to SDS-PAGE and immunoblotted with anti-prohibitin or anti-HSP60 antibody. (C) Mitochondria were purified from growing (Gr) or confluent (Co) cells in 100-mm dishes and subjected to SDS-PAGE, then immunoblotted with an anti-prohibitin or anti-HSP60 antibody. (D) HepG2 cells in six-well plates were transfected with different amounts (μg) of core-expressing plasmid and mitochondrial proteins were analyzed by immunoblotting with anti-prohibitin or anti-HSP60 antibody. The expression levels of the core protein in whole-cell lysates (WCL) were also determined. (E) Cells harboring HCV replicon were untreated or treated with IFN and expression levels of prohibitin in mitochondria were determined. Expression of HCV core and NS5A proteins was also examined. FG, full-genomic replicon cells; SG, subgenomic replicon cells. (F) Expression levels of prohibitin in mitochondria were determined in liver tissues HCV core-gene transgenic and nontransgenic mice. Prohibitin/HSP60 expression levels were determined by densitometry. C-Tg, core-gene transgenic mouse; NT, nontransgenic littermate ($n = 3$) $^*P < 0.05$.

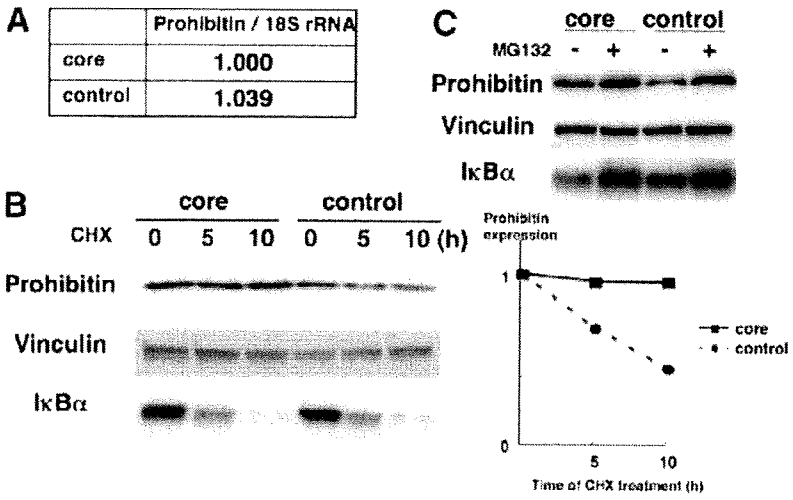

Fig. 3. Increased protein stability of prohibitin in core-expressing cells. (A) RNA was extracted from core-expressing and control cells, and the amount of specific mRNA was determined by real-time PCR with specific primers/probe against prohibitin. The amount of prohibitin mRNA was standardized by that of 18S ribosomal RNA (18S rRNA). (B) Cells were incubated with 100 ng/mL cycloheximide and harvested at the timepoints indicated above the lanes (numbers are hours of cycloheximide treatment). Whole-cell lysates were subjected to SDS-PAGE and immunoblotted with anti-prohibitin, anti-IκBα, or anti-vinculin (as an internal standard) antibody. The intensity of each band was measured by densitometry, and expression levels (prohibitin/vinculin) are shown in the right panel. (C) Cells were harvested after incubation with 20 μM MG132 for 8 hours and subjected to immunoblotting with anti-prohibitin, anti-IκBα, or anti-vinculin antibody.

by immunoblotting (Fig. 2B). Because prohibitin is associated with cell proliferation, it is possible that prohibitin expression changed according to the cell proliferative status. As shown in Fig. 2C, core-expressing cells had high prohibitin expression levels in the cells in both confluent growth and growing statuses compared with control cells. We also determined the expression levels in cells synchronized with aphidicolin followed by l-mimosine treatment and found an increased expression level in core-expressing cells (data not shown). To exclude the possibility that the increased prohibitin expression level is due to the expansion of limited cell clones, not specific to the core protein expression, we examined prohibitin expression in cells transiently expressing the core protein and found that prohibitin expression level increased dose-dependently in core-expressing cells (Fig. 2D). We also examined the prohibitin expression levels in Huh7 cells harboring full- or subgenomic HCV replicon. For this purpose, we used interferon (IFN)-treated replicon cells (cured cells) as a control. Core and nonstructural (NS)5A proteins were not detected after treatment of full-genomic replicon cells with IFN, suggesting a successful elimination of replicon. Prohibitin expression levels in cells with full-genomic replicon were increased compared with those in IFN-treated cured cells, whereas levels of prohibitin expression were low in subgenomic replicon cells regardless of IFN-treatment (Fig. 2E). In addition, prohibitin expression levels were also increased in livers of 3-month-old transgenic mice expressing the core protein compared with those in nontransgenic littermates (Fig. 2F).

We next sought to determine the mechanism of the increased steady-state level of prohibitin in core-expressing cells. To determine prohibitin messenger RNA (mRNA) expression, we performed a real-time polymerase chain reaction (PCR) using specific primers/probe. No difference in prohibitin mRNA was observed between core-expressing and control cells (Fig. 3A). We next determined the stability of prohibitin in these cells. By treating the cells with cycloheximide, the expression levels of prohibitin gradually decreased in control cells (Fig. 3B). On the other hand, in core-expressing cells prohibitin was hardly degraded by cycloheximide treatment for 10 hours, whereas IκBα was equally degraded in both cells. This result suggests that prohibitin was stabilized in the presence of the core protein. Because prohibitin has been shown to be degraded by proteasome,[23] we examined expression levels of prohibitin in the presence of proteasome inhibitor MG132. By treatment with MG132, prohibitin expression was increased to the similar level in core-expressing and control cells. These results suggest that the core protein may inhibit proteasomal degradation of prohibitin by some mechanism, including the prevention of degradation by interaction with the core protein. Then, core-expressing cells were lysed and subjected to immunoprecipitation with an anti-prohibitin antibody. As shown in Fig. 4, the core protein was coimmunoprecipitated with an anti-prohibitin antibody. To exclude a nonspecific interaction with the antibody or Sepharose beads, cells expressing a small amount of prohibitin by transfection with small interfering RNA (siRNA) against prohibitin were also examined. In these cells the amount of the coimmunoprecipitated core protein decreased. In addition, the core protein was not coimmunoprecipitated by control immunoglobulin G (IgG), indicating a specific interaction of prohibitin with the core protein. These results suggest that prohibitin expression increased in core-expressing cells owing to the increased stability presumably by interaction with the core protein.

Impaired Chaperon Function of Prohibitin in Core-Expressing Cells. We next examined the effect of

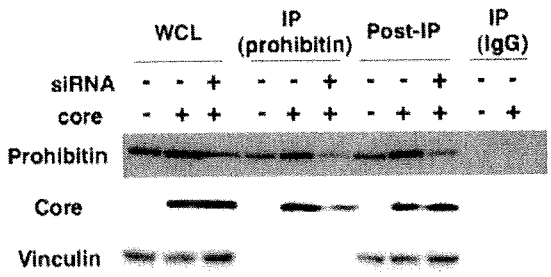

Fig. 4. Interaction of the core protein with prohibitin. Core-expressing and control cells were transfected with or without siRNA against the prohibitin gene, then harvested and lysed in NET-N buffer 3 days after transfection. Whole-cell lysates (WCL) were immunoprecipitated (IP) with an anti-prohibitin antibody or control IgG and immunoblotted with anti-prohibitin or anti-core antibody. Supernatants after the immunoprecipitation were harvested and similarly immunoblotted (Post-IP).

the interaction of prohibitin with the core protein on the function of prohibitin. Prohibitin works as a chaperon of mitochondrial proteins. Nijtmans et al.[21] demonstrated that prohibitin exerts a chaperon function particularly for the stabilization of mitochondrial DNA-encoded proteins. COX is a mitochondrial respiratory complex IV formed by 14 subunits, 10 of which are encoded by nuclear DNA and the rest by mitochondrial DNA.[24] We examined the interaction of prohibitin with subunit II of COX encoded by mitochondrial DNA. As shown in Fig. 5A, the level of COX II coimmunoprecipitated with an anti-prohibitin antibody was decreased in core-expressing cells, although the amount of immunoprecipitated prohibitin was higher than that in control cells. On the other hand, the subunit IV of COX encoded by nuclear DNA was similarly coimmunoprecipitated between core-expressing and control cells. When prohibitin expression was decreased by siRNA transfection, coimmunoprecipitation of COX subunits was similarly decreased with the amount of immunoprecipitation of prohibitin itself being low. We next determined expression levels of COX subunits in the mitochondria in these cells. Expression levels of mitochondrial DNA-encoded subunits I and II in core-expressing cells were decreased, whereas the levels of nuclear DNA-encoded subunits IV and VIb were similar to those in control cells. When transfected with prohibitin-siRNA, expression levels of all of the COX subunits examined were decreased in both core-expressing and control cells, suggesting that protein levels of these subunits are dependent on prohibitin (Fig. 5B, see Supporting Fig. 1 for densitometry). Similar data were observed when blots for COX II and IV were developed together in the same membrane (Supporting Fig. 2). We also determined COX activity in these cells and found that core-expressing cells had a significantly decreased COX activity (about 70% of that in control cells, Fig. 5C). These results suggest that interaction of prohibitin with the core protein is associated with an impaired function of prohibitin as a mitochondrial chaperon, which may trigger disordered assembly and function of mitochondrial respiratory complexes.

Discussion

In the present study we analyzed expression levels of mitochondrial proteins in HepG2 cells expressing the HCV core protein and identified a set of proteins with different expressions. Some of those proteins were related to the mitochondrial respiratory chain (Table 1). Because the core protein was shown to be associated with the induction of oxidative stress,[7-9] the core protein may modulate the expression and function of proteins forming mitochondrial respiratory complexes, which naturally

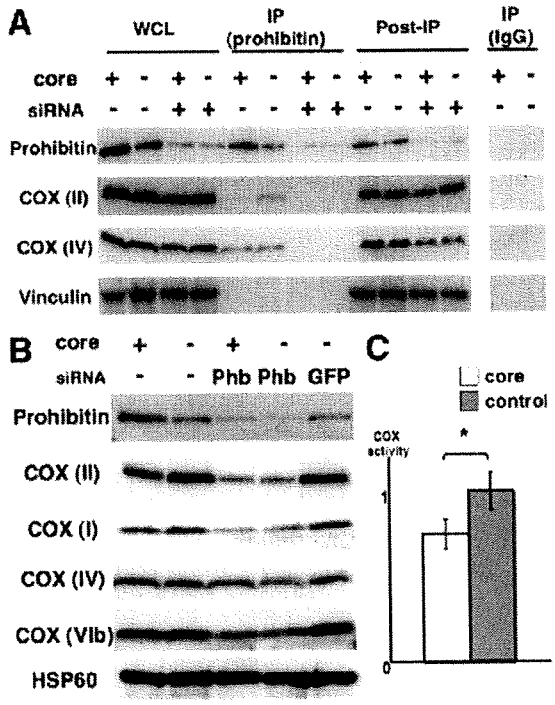

Fig. 5. Effects of core-prohibitin interaction on interaction/expression of COX subunit proteins and COX activity. (A) Whole-cell lysates (WCL) of core-expressing and control cells were subjected to immunoprecipitation with an anti-prohibitin antibody or control IgG, and the interaction of prohibitin with COX subunits was determined by immunoblotting of immunoprecipitated proteins (IP). Supernatants after the immunoprecipitation were harvested and similarly immunoblotted (Post-IP). (B) Cells were transfected with or without siRNA against the prohibitin (Phb) or GFP gene and harvested 3 days after transfection for purification of mitochondria. Purified mitochondria were subjected to SDS-PAGE and immunoblotted with several anti-COX subunits antibodies. The expression levels of HSP60 were also examined as an internal control. (C) COX activity was determined by measuring cytochrome c oxidation. The activity was normalized by taking the average rate of control cells as 1. Data shown are means ± SE ($n = 5$). *$P < 0.05$.

leads to ROS accumulation. In addition, MnSOD, which plays a key role in protecting cells from oxidative damage, was up-regulated in core-expressing cells, reflecting ROS increase in the cells. Several protein chaperons such as HSP70 and GrpE-like protein co-chaperon were also identified as up-regulated proteins. Because these proteins are known to be important in the mitochondrial protein-import mechanisms, the modulated expression of these proteins may be associated with the different expressions of the identified mitochondrial proteins.

Prohibitin, a mitochondrial protein chaperon, was identified as an up-regulated protein in core-expressing cells. Prohibitin is a ubiquitously expressed and highly conserved protein that was originally determined to play a predominant role in inhibiting cell-cycle progression and cellular proliferation by attenuating DNA synthesis.[20,25] Prohibitin is present in the nucleus and interacts with transcription factors that are important in cell cycle progression. In core-expressing cells used in this study, prohibitin was also detected in the nucleus and its expression level was also higher than that in control Hepswx cells or HepG2 cells (data not shown). The growth rate of core-expressing cells, however, was similar to that of control cells (data not shown). The physiological significance of the high expression level of prohibitin in the nucleus remains to be determined, but it may be related to enhanced apoptosis by Fas ligand, as shown by Ruggieri et al.,[16] because prohibitin interacts with E2F, Rb, and p53 and modulates the transcription activity of these factors and induces apoptosis.[26,27]

Mitochondrial prohibitin acts as a protein chaperon by stabilizing newly synthesized mitochondrial translation products through direct interaction.[21] We examined the interaction between prohibitin and mitochondrially encoded subunit II of COX and found a suppressed interaction between these proteins in core-expressing cells. In addition, there are several studies that showed the association of prohibitin with the assembly of mitochondrial respiratory complex I as well as complex IV (COX).[21,28] Complex I also consists of both nuclear- and mitochondrial-DNA-encoded subunits; therefore, it is probable that the assembly and function of complex I are impaired by the core protein. We attempted to examine the interaction of prohibitin with the mitochondrial DNA-encoded subunit of complex I, but commercially available antibodies against this subunit could not detect the protein itself by immunoblotting (data not shown). With respect to the complex I function, we found a decreased complex I activity in core-expressing cells (H. Miyoshi et al., manuscript in preparation). Other groups have also shown that complex I activity is decreased in the liver of transgenic mice harboring HCV core and envelope genes[9] as well as in cultured cells.[29] From these findings, the interaction between prohibitin and the core protein may impair the function of complex I as well as complex IV, leading to an increase in ROS production. In fact, the suppression of the prohibitin function is shown to result in an increased production of ROS,[30] a phenomenon observed in core-expressing cells used in this study (Miyoshi et al., in prep.) as well as in the liver of core-gene transgenic mice.[7,8] Interestingly, Berger and Yaffe[31] showed that loss of function of prohibitin leads to an altered mitochondrial morphology, that is, the loss of the normal reticular morphology and organized mitochondrial distribution. In hepatocytes from the core-gene transgenic mice, we observed a change in morphology of mitochondria, a disappearance of the double structure of mitochondrial membranes.[2] These changes in mitochondrial morphology are somewhat different, but the dysfunction of prohibitin may be responsible for the morphological abnormality of mitochondria observed in the core-gene transgenic mice.

We concluded that prohibitin overexpression is due to increased stability induced by the interaction with the core protein. In this study we showed that prohibitin might be degraded by proteasome, although we could not detect ubiquitinated forms of prohibitin. If the degradation is mediated by ubiquitin as reported,[23] it is possible that the interaction with the core protein interferes with ubiquitin-binding and protects prohibitin from degradation by proteasome. Some posttranslational protein modifications such as phosphorylation are other possible factors for the stabilization, because prohibitin can be serine-phosphorylated[32]; however, in our examination no serine/threonine/tyrosine phosphorylation of prohibitin was detected in core-expressing cells (data not shown). Thus far, there are no studies showing that prohibitin stabilization leads to a suppressed function as a mitochondrial chaperon. Therefore, this finding is novel and noteworthy because the prohibitin expression level has been considered to be proportional to the chaperon function. Prohibitin is highly expressed in several human tumors.[33,34] In addition, a 2D-PAGE of the hepatoma cell line HCC-M identified prohibitin as a positively regulated protein.[35] In these studies, the mechanism of prohibitin overexpression was not elucidated, but considering that prohibitin is associated with the inhibition of cell proliferation, the function of prohibitin is suppressed by stabilization by some molecules in the tumor, similar to the mechanism we suggest in the current study.

In addition to HepG2 cells constitutively expressing the core protein, increased prohibitin expression levels were also found in livers of core-gene transgenic mice.

The difference in expression levels between the transgenic mice and nontransgenic littermates, however, was a little bit smaller than that in the studies of HepG2 cells. This may be due to the low expression level of the core protein in the transgenic mice compared with that in core-expressing HepG2 cells because the expression level of prohibitin was proportionally increased to that of the core protein as shown in this study (Fig. 2D). Otherwise, there might be some *in vivo* mechanism for suppressing prohibitin expression in mice.

In this study, COX subunit IV as well as II were found to interact with prohibitin (Fig. 5A). Although there are no studies demonstrating that prohibitin also works as chaperon for nuclear DNA-encoded mitochondrial proteins as far as we investigated, knockdown of prohibitin expression by siRNA led to decreases in expression levels of both nuclear (COX IV, VIb) and mitochondrial (COX I, II) DNA-encoded subunits in mitochondria (Fig. 5B and Supporting Figs. 1 and 2). We showed that COX IV interacts with prohibitin (Fig. 4), suggesting that prohibitin also works for stable expression of nuclear DNA-encoded COX IV. Degrees of decrease in COX IV and VIb expression, however, were smaller than those in I and II. Prohibitin might contribute to stabilization of COX IV and VIb by mechanism(s) other than chaperon function. Steglich et al.[36] showed that prohibitin regulates protein degradation by the m-AAA protease in mitochondria. Recently, Da Cruz et al.[37] showed that SLP-2, a member of the stomatin gene family, interacts with prohibitin and regulates the expression of mitochondrial proteins such as COX IV and ND6 of complex I encoded by nuclear DNA by AAA proteases. In view of these findings, COX IV and VIb expression in mitochondria is dependent on prohibitin but other factors may also be involved in the attainment of stable expression of these subunits. The expression levels of COX II and IV in the whole-cell lysates were not so drastic among cell samples (Fig. 5A) compared to those in the mitochondria (Fig. 5B). The reason is not clear, but it is possible that redundant proteins such as improperly folded proteins by lack of chaperons were included in the whole-cell lysates.

In summary, we analyzed mitochondrial proteins in core-expressing HepG2 cells by proteomics analysis and identified prohibitin as an up-regulated protein. The dysfunction of prohibitin induced by the core protein may lead to ROS overproduction in the mitochondrion, which plays a key role in the pathogenesis of chronic hepatitis C. The restoration of prohibitin function might be a therapeutic option for correcting the dysregulated assembly and dysfunction of mitochondrial respiratory chain complexes.

Acknowledgment: We thank S. Shinzawa, M. Yahata, and S. Yoshizaki for technical assistance.

References

1. Suzuki R, Suzuki T, Ishii K, Matsuura Y, Miyamura T. Processing and functions of Hepatitis C virus proteins. Intervirology 1999;42:145-152.
2. Moriya K, Fujie H, Shintani Y, Yotsuyanagi H, Tsutsumi T, Ishibashi K, et al. The core protein of hepatitis C virus induces hepatocellular carcinoma in transgenic mice. Nat Med 1998;4:1065-1067.
3. Naas T, Ghorbani M, Alvarez-Maya I, Lapner M, Kothary R, De Repentigny Y, et al. Characterization of liver histopathology in a transgenic mouse model expressing genotype 1a hepatitis C virus core and envelope proteins 1 and 2. J Gen Virol 2005;86:2185-2196.
4. Machida K, Cheng KT, Lai CK, Jeng KS, Sung VM, Lai MM. Hepatitis C virus triggers mitochondrial permeability transition with production of reactive oxygen species, leading to DNA damage and STAT3 activation. J Virol 2006;80:7199-7207.
5. Suzuki R, Sakamoto S, Tsutsumi T, Rikimaru A, Tanaka K, Shimoike T, et al. Molecular determinants for subcellular localization of hepatitis C virus core protein. J Virol 2005;79:1271-1281.
6. Schwer B, Ren S, Pietschmann T, Kartenbeck J, Kaehlcke K, Bartenschlager R, et al. Targeting of hepatitis C virus core protein to mitochondria through a novel C-terminal localization motif. J Virol 2004;78:7958-7968.
7. Moriya K, Nakagawa K, Santa T, Shintani Y, Fujie H, Miyoshi H, et al. Oxidative stress in the absence of inflammation in a mouse model for hepatitis C virus-associated hepatocarcinogenesis. Cancer Res 2001;61:4365-4370.
8. Okuda M, Li K, Beard MR, Showalter LA, Scholle F, Lemon SM, et al. Mitochondrial injury, oxidative stress, and antioxidant gene expression are induced by hepatitis C virus core protein. Gastroenterology 2002;122:366-375.
9. Korenaga M, Wang T, Li Y, Showalter LA, Chan T, Sun J, et al. Hepatitis C virus core protein inhibits mitochondrial electron transport and increases reactive oxygen species (ROS) production. J Biol Chem 2005;280:37481-37488.
10. Diamond DL, Jacobs JM, Paeper B, Proll SC, Gritsenko MA, Carithers RL Jr, et al. Proteomic profiling of human liver biopsies: hepatitis C virus-induced fibrosis and mitochondrial dysfunction. HEPATOLOGY 2007;46:649-657.
11. Moriya K, Yotsuyanagi H, Shintani Y, Fujie H, Ishibashi K, Matsuura Y, et al. Hepatitis C virus core protein induces hepatic steatosis in transgenic mice. J Gen Virol 1997;78(Pt 7):1527-1531.
12. Moriya K, Todoroki T, Tsutsumi T, Fujie H, Shintani Y, Miyoshi H, et al. Increase in the concentration of carbon 18 monounsaturated fatty acids in the liver with hepatitis C: analysis in transgenic mice and humans. Biochem Biophys Res Commun 2001;281:1207-1212.
13. Fujie H, Yotsuyanagi H, Moriya K, Shintani Y, Tsutsumi T, Takayama T, et al. Steatosis and intrahepatic hepatitis C virus in chronic hepatitis. J Med Virol 1999;59:141-145.
14. Cho WC. Contribution of oncoproteomics to cancer biomarker discovery. Mol Cancer 2007;6:25.
15. Lescuyer P, Strub JM, Luche S, Diemer H, Martinez P, Van Dorsselaer A, et al. Progress in the definition of a reference human mitochondrial proteome. Proteomics 2003;3:157-167.
16. Ruggieri A, Harada T, Matsuura Y, Miyamura T. Sensitization to Fas-mediated apoptosis by hepatitis C virus core protein. Virology 1997;229:68-76.
17. Okado-Matsumoto A, Fridovich I. Subcellular distribution of superoxide dismutases (SOD) in rat liver: Cu,Zn-SOD in mitochondria. J Biol Chem 2001;276:38388-38393.
18. Murakami K, Ishii K, Ishihara Y, Yoshizaki S, Tanaka K, Gotoh Y, et al. Production of infectious hepatitis C virus particles in three-dimensional cultures of the cell line carrying the genome-length dicistronic viral RNA of genotype 1b. Virology 2006;351:381-392.

19. Shevchenko A, Wilm M, Vorm O, Mann M. Mass spectrometric sequencing of proteins silver-stained polyacrylamide gels. Anal Chem 1996;68: 850-858.
20. Mishra S, Murphy LC, Murphy LJ. The prohibitins: emerging roles in diverse functions. J Cell Mol Med 2006;10:353-363.
21. Nijtmans LG, de Jong L, Artal Sanz M, Coates PJ, Berden JA, Back JW, et al. Prohibitins act as a membrane-bound chaperone for the stabilization of mitochondrial proteins. EMBO J 2000;19:2444-2451.
22. Back JW, Sanz MA, De Jong L, De Koning LJ, Nijtmans LG, De Koster CG, et al. A structure for the yeast prohibitin complex: structure prediction and evidence from chemical crosslinking and mass spectrometry. Protein Sci 2002;11:2471-2478.
23. Thompson WE, Ramalho-Santos J, Sutovsky P. Ubiquitination of prohibitin in mammalian sperm mitochondria: possible roles in the regulation of mitochondrial inheritance and sperm quality control. Biol Reprod 2003; 69:254-260.
24. Fontanesi F, Soto IC, Horn D, Barrientos A. Assembly of mitochondrial cytochrome c-oxidase, a complicated and highly regulated cellular process. Am J Physiol Cell Physiol 2006;291:C1129-C1147.
25. Mishra S, Murphy LC, Nyomba BL, Murphy LJ. Prohibitin: a potential target for new therapeutics. Trends Mol Med 2005;11:192-197.
26. Fusaro G, Dasgupta P, Rastogi S, Joshi B, Chellappan S. Prohibitin induces the transcriptional activity of p53 and is exported from the nucleus upon apoptotic signaling. J Biol Chem 2003;278:47853-47861.
27. Joshi B, Ko D, Ordonez-Ercan D, Chellappan SP. A putative coiled-coil domain of prohibitin is sufficient to repress E2F1-mediated transcription and induce apoptosis. Biochem Biophys Res Commun 2003;312:459-466.
28. Bourges I, Ramus C, Mousson de Camaret B, Beugnot R, Remacle C, Cardol P, et al. Structural organization of mitochondrial human complex I: role of the ND4 and ND5 mitochondria-encoded subunits and interaction with prohibitin. Biochem J 2004;383:491-499.
29. Piccoli C, Scrima R, Quarato G, D'Aprile A, Ripoli M, Lecce L, et al. Hepatitis C virus protein expression causes calcium-mediated mitochondrial bioenergetic dysfunction and nitro-oxidative stress. HEPATOLOGY 2007;46:58-65.
30. Theiss AL, Idell RD, Srinivasan S, Klapproth JM, Jones DP, Merlin D, et al. Prohibitin protects against oxidative stress in intestinal epithelial cells. FASEB J 2007;21:197-206.
31. Berger KH, Yaffe MP. Prohibitin family members interact genetically with mitochondrial inheritance components in Saccharomyces cerevisiae. Mol Cell Biol 1998;18:4043-4052.
32. Ross JA, Nagy ZS, Kirken RA. The PHB1/2 phosphocomplex is required for mitochondrial homeostasis and survival of human T cells. J Biol Chem 2008;283:4699-4713.
33. Coates PJ, Nenutil R, McGregor A, Picksley SM, Crouch DH, Hall PA, et al. Mammalian prohibitin proteins respond to mitochondrial stress and decrease during cellular senescence. Exp Cell Res 2001;265:262-273.
34. Asamoto M, Cohen SM. Prohibitin gene is overexpressed but not mutated in rat bladder carcinomas and cell lines. Cancer Lett 1994;83:201-207.
35. Seow TK, Ong SE, Liang RC, Ren EC, Chan L, Ou K, et al. Two-dimensional electrophoresis map of the human hepatocellular carcinoma cell line, HCC-M, and identification of the separated proteins by mass spectrometry. Electrophoresis 2000;21:1787-1813.
36. Steglich G, Neupert W, Langer T. Prohibitins regulate membrane protein degradation by the m-AAA protease in mitochondria. Mol Cell Biol 1999; 19:3435-3442.
37. Da Cruz S, Parone PA, Gonzalo P, Bienvenut WV, Tondera D, Jourdain A, et al. SLP-2 interacts with prohibitins in the mitochondrial inner membrane and contributes to their stability. Biochim Biophys Acta 2008;1783: 904-911.

The American Journal of Pathology, Vol. 175, No. 4, October 2009

DOI: 10.2353/ajpath.2009.090102

Immunopathology and Infectious Diseases

Tacrolimus Ameliorates Metabolic Disturbance and Oxidative Stress Caused by Hepatitis C Virus Core Protein

Analysis Using Mouse Model and Cultured Cells

Kyoji Moriya,* Hideyuki Miyoshi,* Takeya Tsutsumi,* Seiko Shinzawa,* Hajime Fujie,* Yoshizumi Shintani,* Hiroshi Yotsuyanagi,* Kohji Moriishi,† Yoshiharu Matsuura,† Tetsuro Suzuki,‡ Tatsuo Miyamura,‡ and Kazuhiko Koike*

From the Department of Internal Medicine, Graduate School of Medicine, University of Tokyo, Tokyo; the Department of Molecular Virology,† Research Institute for Microbial Diseases, Osaka University, Osaka; and the Department of Virology II,‡ National Institute of Infectious Diseases, Tokyo, Japan*

Hepatic steatosis and insulin resistance are factors that aggravate the progression of liver disease caused by hepatitis C virus (HCV) infection. In the pathogenesis of liver disease and metabolic disorders in HCV infection, oxidative stress due to mitochondrial respiratory chain dysfunction plays a pivotal role. Tacrolimus (FK506) is supposed to protect mitochondrial respiratory function. We studied whether tacrolimus affects the development of HCV-associated liver disease using *HCV core gene* transgenic mice, which develop hepatic steatosis, insulin resistance, and hepatocellular carcinoma. Administration of tacrolimus to *HCV core gene* transgenic mice three times per week for 3 months led to a significant reduction in the amounts of lipid in the liver as well as in serum insulin. Tacrolimus treatment also ameliorated oxidative stress and DNA damage in the liver of the *core gene* transgenic mice. Tacrolimus administration reproduced these effects in a dose-dependent manner in HepG2 cells expressing the core protein. The intrahepatic level of tumor necrosis factor-α, which may be a key molecule for the pathogenesis in HCV infection, was significantly decreased in tacrolimus-treated core gene transgenic mice. Tacrolimus thus reversed the effect of the core protein in the pathogenesis of HCV-associated liver disease. These results may provide new therapeutic tools for chronic hepatitis C, in which oxidative stress and abnormalities in lipid and glucose metabolism contribute to liver pathogenesis. ***(Am J Pathol 2009, 175:1515–1524; DOI: 10.2353/ajpath.2009.090102)***

Hepatitis C virus (HCV) is a major cause of liver disease; approximately 170 million people are chronically infected worldwide. Persistent HCV infection leads to the development of chronic hepatitis, cirrhosis, and, eventually, hepatocellular carcinoma (HCC), thereby being a serious problem from both medical and socioeconomic viewpoints.[1,2] Recently, a growing amount of evidence showing that HCV infection induces alteration in lipid[3–7] and glucose metabolism has accumulated.[8,9] Augmentation of oxidative stress is also substantiated in HCV infection by a number of clinical and basic studies.[10–13]

We demonstrated previously that the core protein of HCV induces HCC in transgenic mice that have marked hepatic steatosis in the absence of inflammation.[14] In this animal model for HCV-associated HCC, there is augmentation of oxidative stress in the liver during the incubation period.[10] Also noted is an accumulation of lipid droplets that are rich with carbon 18 monounsaturated fatty acids such as oleic and vaccenic acids, which is also observed in liver tissues of patients with chronic hepatitis C com-

Supported in part by a Grant-in-Aid for Scientific Research on Priority Area from the Ministry of Education, Science, Sports and Culture of Japan, by Health Sciences research grants from the Ministry of Health, Labour and Welfare (Research on Hepatitis), and by the Program for Promotion of Fundamental Studies in Health Sciences of the Organization for Drug ADR Relief, R&D Promotion and Product Review of Japan.

Accepted for publication June 22, 2009.

Address reprint requests to Kazuhiko Koike, M.D., Ph.D., Department of Gastroenterology, Internal Medicine, Graduate School of Medicine, University of Tokyo, 7-3-1 Hongo, Bunkyo-ku, Tokyo 113-8655, Japan. E-mail: kkoike-tky@umin.ac.jp.

pared with those in patients with fatty liver due to simple obesity.[15] Recently, we have also shown, using the HCV transgenic mouse model, that the ability of insulin to lower plasma glucose levels is impaired in association with HCV infection,[16] which would be the basis for the frequent development of type 2 diabetes in patients with chronic hepatitis C.[8,9]

Disturbances in lipid and glucose metabolism are notable features of HCV infection and may be profoundly involved in the pathogenesis of liver diseases. Although the mechanism underlying these phenomena is not yet well understood, the development of clues to correct these metabolic disturbances occurring in HCV infection, which have been recently connected to the poor prognosis of patients with chronic hepatitis C, is awaited. Moreover, a key role for oxidative stress in the pathogenesis of hepatitis C,[11,12] which may be closely associated with the aforementioned metabolic disorders, has been identified. The association of oxidative stress augmentation in HCV infection with mitochondrial respiratory dysfunction[10,13,17] suggests that one possibility to ameliorate such a condition is the use of agents that can protect the mitochondrial respiratory function.

We have conducted information retrieval and screening for agents that can protect the mitochondrial respiratory function. Tacrolimus (FK506), which is widely used in organ transplantation, is one such agent with evidence showing protection of the mitochondrial respiratory function,[18–21] although it shows no antiviral effect. We explored, using transgenic mouse and cultured cell models that express the HCV core protein, whether tacrolimus improves metabolic disturbances including lipid and glucose homeostases as well as oxidative stress augmentation through a possible involvement of mitochondrial function.

Materials and Methods

Transgenic Mouse and Cultured Cells

The production of *HCV core gene* transgenic mice has been described previously.[6] Mice were cared for according to institutional guidelines with the approval by the institutional review board of the animal care committee, fed an ordinary chow diet (Oriental Yeast Co., Ltd., Tokyo, Japan), and maintained in a specific pathogen-free state. Because there is a sex preference in the development of liver lesions in the transgenic mice, we used only male mice. At least five mice were used in each experiment, and the data were subjected to statistical analysis. HepG2 cell lines expressing the HCV core protein under the control of the CAG promoter (Hep39J, Hep396, and Hep397) or a control HepG2 line (Hepswx) carrying the empty vector were described previously.[22,23] Bulk HepG2 cells were also used as a control.

Reagents

Cholesterol esters and lipid standards were purchased from Sigma-Aldrich (St. Louis, MO), and glycogen and amyloglucosidase were obtained from Seikagaku Kogyo (Tokyo, Japan). Other chemicals were of analytical grade and were purchased from Wako Chemicals (Tokyo, Japan). Tacrolimus (FK506) was kindly provided by Astellas Pharma Inc. (Tokyo, Japan). Cyclosporine A (CyA) was purchased from Sigma-Aldrich.

Administration of Tacrolimus and Cyclosporine A

Tacrolimus (0.1 mg/kg b.wt., suspended in mannitol and hydroxychlorinated caster oil [HCO-60]), or vehicle only was administered to the core gene transgenic or control mice i.p., three times per week for 3 months beginning at 3 months of age. For *in vitro* experiments, tacrolimus was added to the culture medium at the final concentration of 0 nmol/L, 10 nmol/L, 100 nmol/L, or 1 μmol/L. CyA was also added to the culture medium at the same concentrations.

Assessment of Glucose Homeostasis

Blood was drawn at different time points from the tail vein, and plasma glucose concentrations were measured using an automatic biochemical analyzer (DRI-CHEM 3000V, Fuji Film, Tokyo, Japan). The levels of serum insulin were determined by radioimmunoassay (Biotrak, Amersham Pharmacia Biotech, Piscataway, NJ) using rat insulin as a standard. For the determination of the fasting plasma glucose level, the mice were fasted for >16 hours before the study. An insulin tolerance test was performed as described previously.[16]

Lipid Extraction, Measurement of Triglyceride Content, and Analysis of Fatty Acid Compositions

Lipid extraction from the mouse liver tissues or cultured cells was performed as described previously.[15,24] For the analysis of fatty acid compositions, the residue was methanolysed by the modified Morrison and Smith method with boron trifluoride as a catalyst.[25] Fatty acid methyl esters were analyzed using a Shimadzu GC-7A gas chromatograph (Shimadzu Corp., Kyoto, Japan) equipped with a 30-m-long × 0.3-mm diameter support coated with ethylene glycol succinate.[24]

Evaluation of Oxidative and Antioxidative System

Lipid peroxidation was estimated spectrophotometrically using thiobarbituric acid-reactive substances and is expressed in terms of malondialdehyde formed per milligram protein. Reduced glutathione and oxidized glutathione levels were measured as described previously.[10] The total amount of glutathione was calculated by adding the amounts obtained for glutathione and oxidized glutathione. For the evaluation of DNA damage in cells, apurinic/apyrimidinic sites were determined using a DNA Damage Quantification Kit (Dojindo Molecular Technolo-